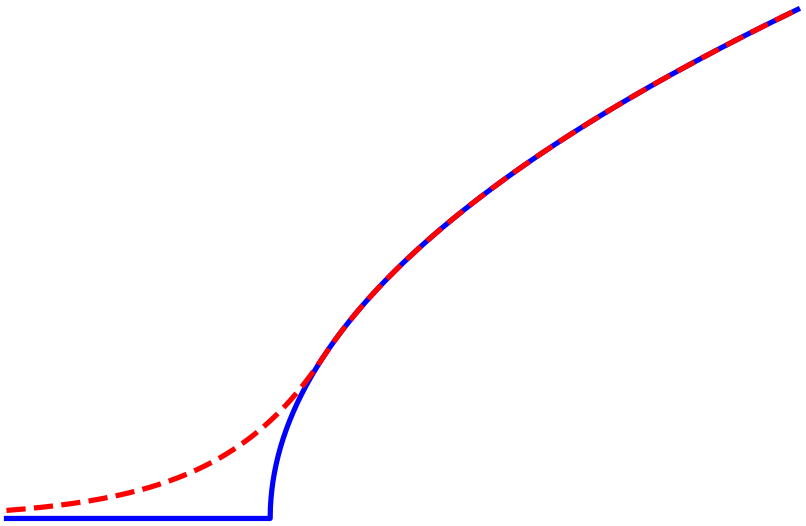

Band Tails and Disordered Potentials

Theoretical investigation of how the structure of electronic bands affects the exponential tail of the density of states.

Master's thesis in Physics

Alexandru Golic

Department of Physics
CHALMERS UNIVERSITY OF TECHNOLOGY
UNIVERSITY OF GOTHENBURG
Gothenburg, Sweden 2023

Master's thesis 2023

Band Tails and Disordered Potentials

Theoretical investigation of how the structure of electronic bands affects the exponential tail of the density of states.

Alexandru Golic

UNIVERSITY OF
GOTHENBURG

CHALMERS
UNIVERSITY OF TECHNOLOGY

Department of Physics
Chalmers University of Technology
University of Gothenburg
Gothenburg, Sweden 2023

Band Tails and Disordered Potentials
Theoretical investigation of how the structure of electronic bands affects the exponential tail of the density of states.
Alexandru Golic

Supervisor: Johannes Hofmann, Department of Physics, University of Gothenburg
Examiner: Ulf Gran, Department of Physics, Chalmers University of Technology

Master's Thesis 2023
Department of Physics
Chalmers University of Technology and University of Gothenburg
SE-412 96 Gothenburg
Telephone +46 31 772 1000

Cover: Schematic view of the band tail in the density of states of a solid arising from a disorder potential. The blue line shows the density of states without disorder, while the dotted red line shows the density of states with disorder.

Typeset in LaTeX
Gothenburg, Sweden 2023

Band Tails and Disordered Potentials
Theoretical investigation of how the structure of electronic bands affects the exponential tail of the density of states.
Alexandru Golic
Department of Physics
Chalmers University of Technology and University of Gothenburg

Abstract

It has long been known that the density of states in a semiconductor decays exponentially into the gap. This tail in the density of states is caused by impurities in the atomic lattice that creates localized states with energies in the gap region. By modeling the impurities as a correlated Gaussian disorder potential, it is possible to utilize path integrals to calculate the density of states in the tails. In this thesis, I examine how the form of the dispersion relation of the band affects the band tail when compared to a standard parabolic dispersion $|\mathbf{k}|^2$. I find that for monomial dispersions $|\mathbf{k}|^q$ with powers higher than $q = 2$ there does not exist any region with a purely exponential decay, only regions where it decays quicker. For double-well dispersions I find that the density of states decays in a slightly different, but still comparable way to monomial dispersion.

Keywords: Physics, band gaps, electrons, path integrals, solids, band tails.

Acknowledgements

First of all I would dearly like to thank my supervisor Johannes Hofmann for all the guidance he has given me in this project. In particular his advice on how to structure a larger project such as this has proven invaluable. I would also like to thank my friends and family, especially my fellow members of the Jungle Patrol, who have given me much appreciated support during the year.

Alexandru Golic, Gothenburg, 2023-06-12

Contents

1

Introduction

1.1 Background

The advent of quantum theory in the early 1900's allowed for the explanation of many phenomena that previously had not been understood. In the case of the electric properties of solids, the leading classical description was the Drude model. In this model, electrons are described as moving randomly inside a solid without interacting or colliding with each other, and only interacting with the atomic nuclei through collisions. Although these assumptions were somewhat dubious in the context of classical physics this model had great success in explaining many of the electric properties of solids.

A full quantum description of the problem can first be credited to Bloch. By approximating the solid as an infinite periodic crystal, and assuming that the interactions of all electrons with the atomic nuclei and each other can be modelled by an effective potential, Bloch showed that the electrons in a solid do not scatter in the lattice but instead diffract, with the electronic states being delocalised over the whole solid.

This way of describing solids also reveals an interesting property: The density of states of a solid will in general consist of regions where it is non-zero (called bands) and regions where it vanishes (called gaps). Due to the Pauli exclusion principle, which states that no two electrons can occupy the same quantum state, in the lowest energy configuration the electrons will "fill up" the available states from the lowest possible energy up to some maximum energy called the Fermi energy E_{F}.

Depending on the position of the Fermi energy it is possible to make a rough split of solids into two categories. In metals the Fermi energy lies inside of an energy band, and thus there will exist empty states with infinitesimally larger energy than the highest energy electrons. This makes the electrons easily excited by an external electric field which allows them to conduct electricity.

In semiconductors on the other hand the Fermi energy generally lies in the gap between the first band (the valence band) and the second band (the conduction band). This means that the electrons at zero temperature have energies only in the valence band. To excite them thus requires a large enough energy to overcome the band gap, and so they essentially get locked into place inside the valence band. At non-zero temperatures however some electrons will be excited into the conduction band due to thermal effects. Since these electrons will have empty states with

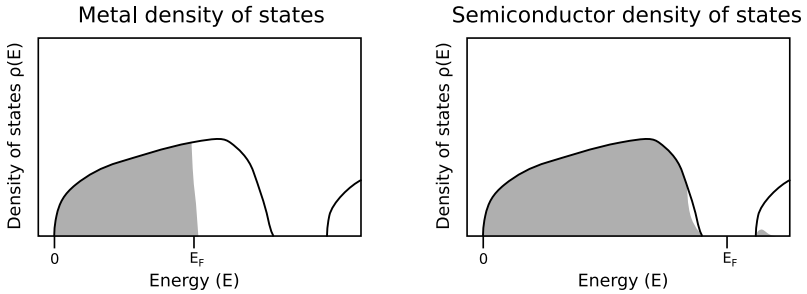

Figure 1.1: Schematic comparison of the filled density of states for metals and semiconductors respectively. The shaded areas indicate what states are occupied by the electrons at some non-zero temperature and E_F denotes the Fermi energy.

infinitesimally larger energies they will be able to conduct electricity, and likewise will the "holes" they leave behind in the valence band. These two cases are visualized in Figure 1.1.

Although this way of describing the electrons gives very good qualitative predictions of the electronic properties of solids, not all predictions match with experiments. One example of this is the edges of the bands. While the model of diffracting electrons predicts a sharp edge between the band and gap regions, experiments show a different result.

In the beginning of the 1950's, Urbach showed evidence of an exponential tail in the optical absorption in ionic crystals [1]. Further research showed that these tails were universal in solids, and were linked with an exponential tail in the density of states [2]. This was understood to arise from impurities in the lattice which create localized states with energies in the gap region. In recent years it has been shown that these band tails can negatively affect the performance of both transistors [3] and photovoltaic cells [4], and thus understanding them is of great interest.

A method that has been used to analyze band tails theoretically is to model the electrons at the bottom of the bands as free electrons with an effective mass depending on the curvature of the band at its minimum. One can then view the effect of the lattice impurities as a random potential creating local bound states for the electrons. The average density of states for such a system can then be calculated using path integrals [2].

The effective mass approximation on which much of the previous literature rests is however based on the assumption that the dispersion relation at the conduction band minimum is isotropic and parabolic. This need not be the case. A prominent example of a material which does not follow this pattern is multi-layered graphene with a dispersion relation on the form $|\mathbf{k}|^q$, with $q = 1, 2, ...$ [5]. Furthermore, materials may have band structures with multiple minima. Although the effects of different correlations has been previously studied [6] no one has yet investigated other dispersion relations than parabolic ones.

1.2 Aims and Results

The aim of this thesis is to investigate how different dispersion relations affect the band tail when compared to a parabolic dispersion. Specifically, I will look at band structures with a monomial dispersion relation $|\mathbf{k}|^q$, as in multi-layer graphene, as well as band tails with multiple minima, where I will focus on the simple case when the dispersion relation is given by $\mu k^4 - \gamma k^2$.

The central results are that monomial dispersions with $q > 3$ do not seem to contain any energy regions where the decay is approximately exponential, only regions where it decays quicker. For the simple double well dispersion $\mu k^4 - \gamma k^2$, I also see a slightly wider tail than for simple parabolic dispersions γk^2.

2

Theory

In this chapter I will discuss the theoretical background of the problem and how to formulate it analytically. The central aim of this thesis is to calculate the band tails of a solid with impurities and investigate how the shape of the band structure affects this result.

This is a complicated question that can be split into several steps. First is the question of how one can represent this system. Under the assumption that the dynamics are well-described by quantum mechanics, this means finding the Hamiltonian that governs the movement of the electrons. This is explained in more detail in chapter 2.1, but it can be summarized as follows:

I first assume that the solid can be described as a crystal with impurities. In a perfect crystal the electronic states are described by Bloch wavefunctions $\psi_n(\mathbf{x}) = u_n(\mathbf{x})e^{i\mathbf{k}_n\cdot\mathbf{x}}$, where n labels the different eigenstates, $u_n(\mathbf{x})$ is a lattice-periodic function and $\mathbf{k}_n$ is the crystal momentum of the state. Writing the energy in each band as a function of the crystal momentum gives a dispersion relation $\mathcal{E}(\mathbf{k})$.

Although these states are bound in the solid, one can approximate the states at the bottom of the bands as being free states with momentum $\mathbf{k}$ and a "kinetic energy" given by $\mathcal{E}(\mathbf{k})$. If the band is approximately parabolic at its minimum, the dispersion relation will be $\mathcal{E}(\mathbf{k}) \propto |\mathbf{k}|^2$, which is identical to the dispersion of the free particle with a mass proportional to the inverse of the band curvature. This need not be the case however, and it is through this dispersion relation that the band structure affects our calculations.

Since the impurities in the crystal will be randomly distributed, I assume that they can be modeled as a random disorder potential on top of the periodic ones from the crystal. I will also assume that this potential is correlated with a characteristic correlation length λ_0. Assuming that the random potential is weak enough, the band structure is expected to remain mostly intact. Due to the disorder potential however, new localized bound states will appear. Since I assume that the band structure remains the same, at the bottom of the bands the electrons will still behave as free particles with kinetic energy $\mathcal{E}(\mathbf{k})$, with the disorder potential creating new possible bound states.

Once the Hamiltonian of the system in hand the next question naturally follows, namely how one can extract the density of states from this, which is the content of sections 2.3 and 2.4. Since I assume that the disorder potential comes from

impurities in the lattice the correlation length λ_0 will be roughly on the order of the lattice parameter. In a sample of the material that is much larger than this, the density of states can be approximated by the average density of states over all disorder configurations.

Finding the density of states for any particular configuration of the disorder potential is however quite a formidable problem, so taking the average is not straightforward. One way of analytically expressing it however is using path integrals. With this method one can express the average as a path integral over all possible configurations of disorder potential and one can express the density of states for any given configuration as a path integral over a set of replica fields. This will be discussed in more details in Section 2.3.

For energies that are deep enough in the tail (i.e for large $-E$) the path integral can be approximated by their instanton solutions, that is the saddle points of the path integrals. These can be interpreted as the most likely bound states with the given energy.

2.1 Quantum mechanics and Solid State Physics

In this section I will briefly review the quantum mechanics and solid dynamics used in this thesis. Since I assume the reader is already familiar with these topics I will keep it short and try to highlight the arts that are relevant for this work. Subsection 2.1.1 on quantum mechanics is based on the book "Modern Quantum Mechanics" by J.J. Sakurai and J. Napolitano [7], while subsection 2.1.2 is based on the book "Solid State Physics" by P. Hofmann [8].

2.1.1 Quantum mechanics

This subsection reviews the quantum mechanics used in this thesis.

In quantum mechanics the state of a system is described by a vector $\psi(t)$ belong to some complex Hilbert space $\mathcal{H}$, with unit norm $||\psi(t)||^2 = 1$. The state of the system evolves through time according to the Schrödinger equation

$$i\hbar\frac{\partial}{\partial t}\psi(t) = H\psi(t), \tag{2.1}$$

where $\hbar$ is Planck's reduced constant and H the Hamiltonian of the system. The eigenvalues E_n of the Hamiltonian set the possible energies of the system, with corresponding eigenstates ψ_n (known as stationary states) satisfying

$$H\psi_n = E_n\psi_n. \tag{2.2}$$

For a single free particle the Hamiltonian is given by

$$H(\mathbf{x}) = -\frac{\hbar^2}{2m}\nabla^2, \tag{2.3}$$

and for a single particle moving in a potential $V(\mathbf{x})$ the Hamiltonian is given by

$$H(\mathbf{x}) = -\frac{\hbar^2}{2m}\nabla^2 + V(\mathbf{x}), \tag{2.4}$$

although in systems with different moving and interacting particles the Hamiltonian can quickly become much more complicated.

In electronics another useful quantity is the density of states of the systems. The density of states is a function $\rho(E)$ that quantifies the number of energy eigenstates with the energy E per unit of volume. For any energy interval (E_a, E_b) the number of states per volume with energies is given by

$$\int_{E_a}^{E_b} \mathrm{d}E\rho(E). \tag{2.5}$$

For finite-dimensional Hilbert spaces the energy spectrum is given by the discrete and finite eigenvalues of the Hamiltonian, so for a system occupying the volume V_d the density of states is simply

$$\rho(E) = \frac{1}{V_d}\sum_n \delta(E - E_n). \tag{2.6}$$

For continuous systems the situation is sometimes more complicated. Consider for example the free Schrödinger equation

$$H(\mathbf{x})\psi(\mathbf{x}, t) = -\frac{\hbar^2}{2m}\nabla^2\psi(\mathbf{x}, t). \tag{2.7}$$

In this case, the "eigenstates" are given by functions of the form

$$\psi_{\mathbf{k}}(\mathbf{x}) \propto e^{i\mathbf{k}\cdot\mathbf{x}}. \tag{2.8}$$

with energy $E_{\mathbf{k}} = \hbar^2|\mathbf{k}|^2/2m$ and momentum $\hbar\mathbf{k}$. Note however that these eigenfunctions are strictly speaking not states, since they have infinite norm. This also results in a continuous spectrum of energy so Eq. 2.6 stops making sense. Furthermore, since all eigenstates are delocalized over the whole space which has an infinite volume, dividing by the volume of the space is also dubious.

One way of solving this is by considering particles moving inside a box with side length L with periodic boundary conditions. Although this still gives eigenfunctions of the same form as in Eq. 2.8 the periodic boundary conditions impose a constraint on $\mathbf{k}$, with the only allowed values being

$$\mathbf{k} = (k_1, k_2, ..., k_d) = \frac{2\pi}{L}(n_1, n_2, ..., n_d), \tag{2.9}$$

where $k_1, k_2, ...k_d$ label the components of $\mathbf{k}$ and $n_1, n_2, ..., n_d$ are integers.

While this still gives an infinite number of energies, they are now discrete, so Eq. 2.6 can still be applied. When L is large however, the states will be closely spaced together in $\mathbf{k}$-space, so the number of states in spherical shell at radius k with

width dk can be approximated by the volume of the shell. Calculating this in three dimensions (see e.g [7] chapter 2.5) the density of states is approximately

$$\rho(E) \approx \begin{cases} \frac{m^{3/2}E^{1/2}}{\sqrt{2}\pi^2\hbar^3}, & \text{for } E \geq 0, \\ 0, & \text{for } E < 0 \end{cases}. \tag{2.10}$$

In the limit when $L \to \infty$ this identity becomes exact, that for infinite systems the density of states becomes a regular function (i.e not a delta function) of the energy.

2.1.2 Band structures

In this section, I will summarize the relevant parts of solid state mechanics used in this thesis. Specifically, I will highlight the theory behind band structures in solids.

The band structures of solids can be understood by considering a simplified model for the dynamics of the electrons, with two main assumptions. First, I assume that the nuclei form an infinite crystal (that is an infinite periodic lattice), and whose dynamics does not affect the electrons. Second, I assume that for each electron, the total effect of the interactions with the nuclei and other electrons can be summarized in an effective lattice-potential $U(\mathbf{x})$.

Thus the Hamiltonian for each electron becomes

$$H(\mathbf{x}) = -\frac{\hbar^2}{2m}\nabla^2 + U(\mathbf{x}), \tag{2.11}$$

with the added condition that $U(\mathbf{x})$ be lattice-periodic. The solution to such equations are Bloch wavefunctions. These have the form

$$\psi_{\mathbf{k}}(\mathbf{x}) = u_{\mathbf{k}}(\mathbf{x})e^{i\mathbf{k}\cdot\mathbf{x}}, \tag{2.12}$$

where $u_{\mathbf{k}}(\mathbf{x})$ is a lattice-periodic amplitude. Although this form is very reminiscent of the solutions to the free Schrödinger equation 2.8 there are important differences. First, while the different values of the wave vector $\mathbf{k}$ for the free Schrödinger equation all define unique states, for Bloch wavefunctions two states with wave vectors $\mathbf{k}, \mathbf{k}'$ separated by a reciprocal lattice vector are identical. The quantity $\hbar\mathbf{k}$ for the free Schrödinger equation is the momentum, but since states of the states this interpretation fails, and it is instead known as the crystal momentum.

Furthermore in the free Schrödinger equation the energy for a state with wave vector $\mathbf{k}$ is $\hbar^2|\mathbf{k}|^2/2m$. The relationship between the wave vector and the energy of a state is known as a dispersion relation, so for the free Schrödinger equation the dispersion relation is quadratic $\mathcal{E}(\mathbf{k}) \propto |\mathbf{k}|^2$. The dispersion relation for Bloch states is in general much more complicated; as noted before the states themselves are periodic in the wave vector and on top of this there are in general multiple states with the same wave vector in different bands.

This complicated dispersion relation is usually called the band structure of the solid, and can be split into two cases. The first case is metals which have a continuous

density of states starting from the lowest energy state, and the second case is semiconductors/insulators which have energy intervals where the density of states is zero, known as band gaps.

Electrons are fermions, and thus a maximum of two electrons can occupy the same Bloch state (one with spin up and one with spin down). In a solid then the electrons will populate the bands starting from the lowest possible enery up to some highest energy called the Fermi energy E_F. In metals there will always be empty states with infinitesimally more energy than the highest energy electrons. Therefore the electrons are easily excited, for example by an external voltage, and therefore conduct electricity. In semiconductors however the electrons will completely fill up the lowest energy band (known as the valence band) so to reach the next available state in the next band (the conduction band) they need a large enough excitation to overcome the gap. This means that the electrons are harder to excite, and they remain largely unaffected by external voltages, leading to poor conductivity.

At finite temperature however thermal effects ensure that some electrons will be excited from the valence band into the conduction band. Since the conduction band is mostly empty these electrons will be easily excited and thus conduct electricity. These electrons will also, again due to thermal effects, mostly be concentrated around the bottom of the conduction band. As long as they remain at energies close to the bottom of the band, one can treat these electrons as free particles with a kinetic energy given by the dispersion relation $\mathcal{E}(\mathbf{k})$. Even though the dispersion relation as noted before is very complicated (and the fact that it is periodic), for low energy electrons these states are never relevant.

In particular, if the dispersion relation is approximately parabolic at the bottom of the band $\mathcal{E}(\mathbf{k}) \propto |\mathbf{k}|^2$, they will be described by the normal free Schrödinger equation 2.3, but with an effective mass

$$m^* = \hbar^2 \left(\nabla_{\mathbf{k}}^2 \mathcal{E}(\mathbf{k}) \right)^{-1}. \tag{2.13}$$

This is not always the case since there are examples of non-parabolic bands. A famous example is graphene, which has a linear dispersion relation. In these cases the concept of an effective mass does not apply, so I will have to work with the dispersion relation directly.

2.2 Electrons in a random potential

As I noted earlier, the electrons at the bottom of the conduction band behave approximately as free electrons with a kinetic energy given by the dispersion relation $\mathcal{E}(\mathbf{k})$. These equations of motion were derived under the assumption that the solid under consideration was a perfect crystal. In practice however, all solids contain impurities (and semiconductors in particular often do so by design [8]). One can model these impurities as a random disorder potential $V(\mathbf{x})$ added on top of the effective lattice-periodic potential $U(\mathbf{x})$. If this disorder potential is small enough, arguments used in the previous section to still mostly hold. In this case then, the

electrons will still have a kinetic energy given by the dispersion relation at the bottom of the band, but they will no longer be free and instead move in the random potential. As I will show in section 2.4, this gives rise to an exponential tail in the density of states through the appearance of localised bound states.

This exponential decay also motivates why I am only interested in states close to the bottom of the conduction band. Although there might in principle exist tails coming from other parts of the band, the exponential decay means that they quickly become vanishingly few in number compared to the already existing Bloch states in the band. The only bound states that can be measured then are precisely those with energies in the band gap, i.e below the bottom of the band.

Before going into detail of how one can calculate the band tails it is instructive to first consider qualitatively how they arise. In the following discussion I will assume for simplicity that the dispersion relation is parabolic, so the electrons will move according to the standard free Schrödinger equation with some effective mass m. This is what most papers dealing with the problem until now have assumed, but I will show in later chapters how it can be extended to more general dispersions. Also, while the states at the bottom of the conduction band in general do not have zero energy, shifting all energy levels by the same amount does not change the dynamics of a quantum system. Therefore, I will simply take it to be zero. Similarly a nonzero mean of the disorder potential $V(\mathbf{x})$ will shift all energy levels by a constant, so I will set it to zero as well. The electrons at the bottom of the band can thus be approximated as free electrons moving in a random potential $V(\mathbf{x})$ with a zero mean.

As noted in Eq. 2.10, the density of states for a free electron in 3D is given by $\rho(E) \propto \sqrt{E}$ for positive energies and 0 otherwise. Now, consider what happens when the electron instead moves in the disorder potential $V(\mathbf{x})$, which I take to be a correlated Gaussian. If the correlation length is of comparable size to the size of the system, most instances of this potential will have only one or two valleys were bound states can form, as illustrated in Figure 2.1a. This will create bound states for the electrons, as illustrated in Figure 2.1b, but these will be few in number and importantly their energies will be heavily dependent on the particular instance of the disorder potential.

As the correlation length decreases, the number of valleys in the potential grows, as illustrated in Figure 2.1c, and accordingly so does the number of bound states, as illustrated in Figure 2.1d. Finally, when the correlation length is much smaller than the size of the system, as illustrated in Figure 2.1e the density of states can be approximated as a normal function, see Figure 2.1f. Importantly, since the value of the potential at a point is independent of all but its closest neighbours, the density of states can be approximated as the average density of states over all possible configurations. Writing the density of states for a particular disorder configuration as $\rho_V(E)$ gives

$$\rho_V(E) \approx \langle \rho_V(E) \rangle \equiv \rho(E), \tag{2.14}$$

where $\langle . \rangle$ is the average over all disorder potentials.

In this case, I assume that the disorder potential arises from impurities in the lattice. According to [9], the lattice constant for most metals and semiconductors are less than 1 nm, so the correlation length will roughly be on the scale of 1 nm. A conservative estimate is thus that the density of states can be approximated as being continuous for objects with a length of 1 µm or larger, which covers all macroscopic systems.

2.3 Toy Model for Disordered Tails

Before explaining how to use path integrals to calculate the average density of states it is instructive to first consider a (spatially) zero-dimensional toy model. Here, I consider wavefunctions ψ that only exist at a single point, and are thus described by a one-dimensional Hilbert space or equivalently a single complex number. Since Hermitian operators on 1D vector spaces are real numbers, the Hamiltonian will also be some real number $H \in \mathbb{R}$, which must be equal to the (single) energy level of the system. Remember that in the real problem I want to solve, the Hamiltonian can be split into kinetic and potential terms. To anticipate this, I will write the Hamiltonian for this system as two terms as well

$$H^V = H_0 + V, \tag{2.15}$$

where H_0 is the kinetic part and V the potential. Keeping H_0 fixed the energy of the system can now be seen as depending on the potential $E_0^V = H_0 + V$. Taking the volume of the system to be 1, the density of states of this system will then simply be

$$\rho_V(E) = \delta(E - E_0^V). \tag{2.16}$$

Now I will look at a system with a random potential. In particular I will assume that the potential V is a Gaussian random variable with zero mean and variance w^2, i.e $V \sim \mathcal{N}(0, w^2)$. This again anticipates my ansatz for the path integral, and I will discuss more about this particular choice of random distribution later.

Averaging the density of states over the disorder potential gives us

$$\rho(E) \equiv \langle \rho_V(E) \rangle = \frac{1}{\sqrt{2\pi w^2}} \int \mathrm{d}V \rho_V(E) e^{-\frac{V^2}{2w^2}}. \tag{2.17}$$

This simple example can be calculated exactly using Eq. 2.16, and the result is

$$\rho(E) = \frac{1}{\sqrt{2\pi w^2}} \exp\left[-\frac{(H_0 - E)^2}{2w^2} \right]. \tag{2.18}$$

In this case, the average density of states will also be Gaussian, with the same width as the probability distribution for V, although the distribution is shifted by H_0. The interpretation here is simple. Since the only available state has the energy $H_0 + V$ the probability distribution for this single energy level will be the same as for V.

One major difference between this example and higher dimensions is that the Gaussian tail extends in both directions, while the band tails in real solids only extends

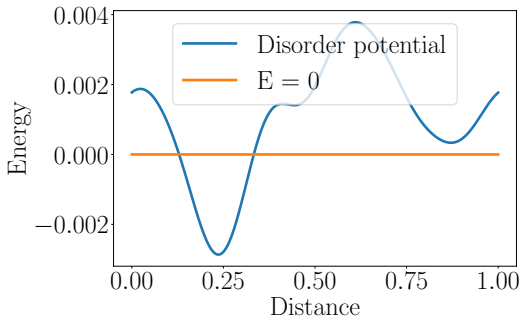

(a) Instance of a disorder potential with a large correlation length.

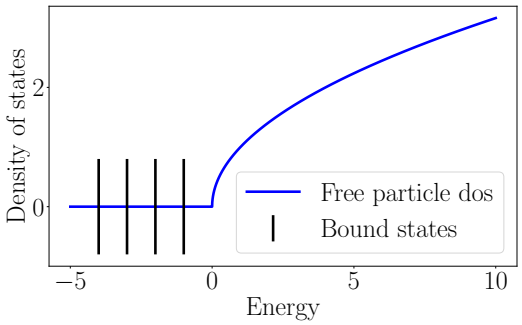

(b) Schematic view of the density of states for a particle moving in the potential in Figure 2.1a.

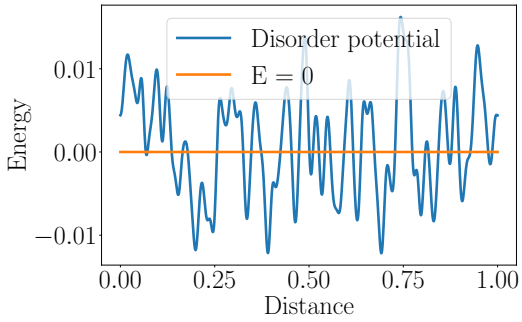

(c) Instance of a disorder potential with a medium correlation length.

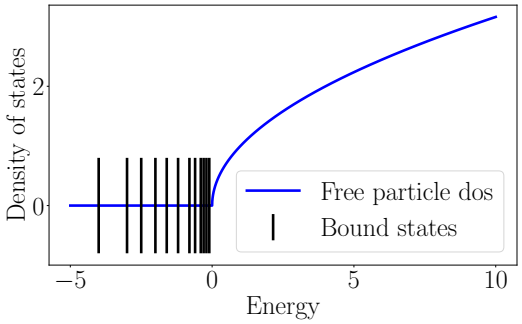

(d) Schematic view of the density of states for a particle moving in the potential in Figure 2.1c.

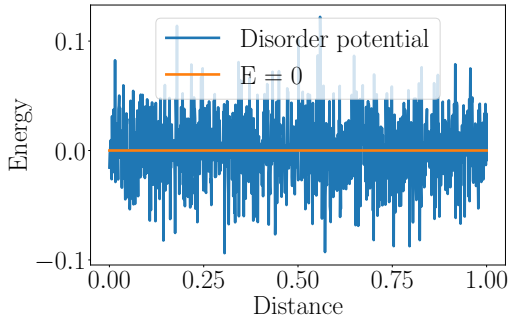

(e) Instance of a disorder potential with a very small correlation length.

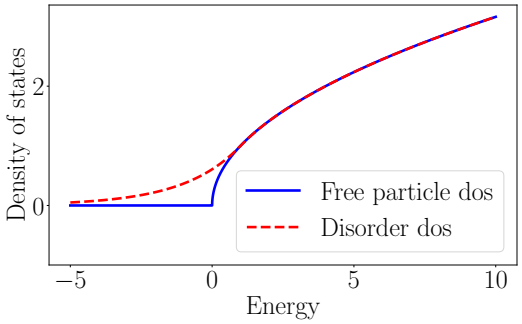

(f) Schematic view of the density of states for a particle moving in the potential in Figure 2.1e. Here the number of states is large enough that the density of states can be approximated by a regular function.

below the bands. The reason for this difference is that in a real solid, there are many possible Bloch states in the band, while the comparatively few states in the gap arise only from bound states created by the disorder potential. In this zero-dimensional case there exists only a single bound state and no continuum of free states, so the band tail extends in both directions.

For problems with higher dimension calculating the average density of states will no longer work, since there is no analytical expression for the density of states of a general potential. A different way of calculating it is to rewrite the density of states using a Gaussian integral. To do this I introduce the partition function

$$\mathcal{Z}_V(E) \equiv \sqrt{\frac{1}{E_0^V - E}}. \tag{2.19}$$

Using the identity

$$\delta(x) = \lim_{\epsilon\to 0}\left(-\frac{1}{\pi}\right)\mathrm{Im}\frac{1}{x+i\epsilon} \tag{2.20}$$

and the fact that

$$\begin{aligned} &2\frac{\partial}{\partial E}\log \mathcal{Z}_V(E) \\ &= 2\frac{\partial}{\partial E}\log(E_0^V - E)^{-1/2} \\ &= -\frac{\partial}{\partial E}\log\{E_0^V - E\} = \frac{1}{E_0^V - E} \\ &= -\frac{1}{E - E_0^V}, \end{aligned} \tag{2.21}$$

one arrives at

$$\rho_V(E) = \delta(E - E_0) = \lim_{\epsilon\to 0}\frac{2}{\pi}\mathrm{Im}\frac{\partial}{\partial E}\log \mathcal{Z}_V(E + i\epsilon). \tag{2.22}$$

The average density of states is then given by

$$\rho(E) = \langle\rho_V(E)\rangle = \lim_{\epsilon\to 0}\frac{2}{\pi}\mathrm{Im}\frac{\partial}{\partial E}\langle\log \mathcal{Z}_V(E + i\epsilon)\rangle = \lim_{\epsilon\to 0}\frac{2}{\pi}\frac{\partial}{\partial E}\mathrm{Im}\langle\log \mathcal{Z}_V(E + i\epsilon)\rangle\,. \tag{2.23}$$

All in all one can rewrite the density of states in terms of the new partition function but so far is not easier to calculate than the original formulation. The advantage of the partition function is that it can be written as a Gaussian integral. This is beneficial since integration over multidimensional Gaussian integrals can easily be performed analytically, and since the average over the disorder potential is also done through a Gaussian integral, the resulting double integral can be treated analytically. While this is superfluous for this zero-dimensional example, this method is more generalizable for higher dimensions.

2.3.1 Replica trick

As I showed in the previous section, the density of states is related to the average of the logarithm of the partition function $\langle\log \mathcal{Z}_V\rangle$, the so called quenched average.

The partition function itself and its average can be expressed in an analytically convenient way, even for higher-dimensional theories, but this is not the case for the logarithm of the partition function.

One way to circumvent this problem is by using the replica trick, which states that for a random variable X

$$\langle \log X \rangle = \lim_{n \to 0} \frac{\langle X^n \rangle - 1}{n}. \tag{2.24}$$

The idea behind this trick is quite simple. Given some random variable X over some domain Ω with a probability density function p and assuming that p is a well-behaved function one can write

$$\begin{aligned} \lim_{n \to 0} \frac{\langle X^n \rangle - 1}{n} &= \lim_{n \to 0} \int_\Omega \mathrm{d}x \frac{x^n - 1}{n} p(x) = \int_\Omega \mathrm{d}x \lim_{n \to 0} \frac{x^n - 1}{n} p(x) \\ &= \int_\Omega \mathrm{d}x \log x \, p(x) = \langle \log X \rangle . \end{aligned} \tag{2.25}$$

Although this is well-defined for real n, it is only feasible to calculate $\langle \mathcal{Z}^n \rangle$ for integer n. Taking the continuous limit in this case then seems more dubious. The method has however been successfully used multiple times in the context of thermodynamics, so I will also use it. For more discussion regarding the validity of the replica trick as well as some examples where it is used, see e.g [10].

2.3.2 Average of one copy of the partition function

Using the replica trick one can skip calculating the logarithm in Eq. 2.23 and instead replace it with $\mathcal{Z}_V^n$. Before tackling the full expression, I will show how one can calculate the simpler quantity $\mathrm{Im} \langle \mathcal{Z}_V(E + i\epsilon) \rangle$. From the definition of the partition function it is clear that it can be written as a Gaussian integral

$$\begin{aligned} \mathcal{Z}_V(E) =& \sqrt{\frac{1}{E_0 - E}} = \sqrt{\frac{1}{H_0 + V - E}} \\ &= \int_{-\infty}^{\infty} \frac{\mathrm{d}\phi}{\sqrt{2\pi}} \exp\left[-\frac{1}{2}(H_0 + V - E)\phi^2 \right], \end{aligned} \tag{2.26}$$

provided that $H_0 + V - E > 0$. When taking the average of this however this is integrated over all values of V, which must include values for which $H_0 + V - E < 0$. This will give rise to a divergent expression, but it is possible to make it converge, as I will show shortly.

Writing the partition function in this way makes it easy to take the average.

$$\langle \mathcal{Z}_V(E) \rangle = \int \mathrm{d}V \sqrt{\frac{1}{2\pi w^2}} \int_{-\infty}^{\infty} \frac{\mathrm{d}\phi}{\sqrt{2\pi}} \exp\left[-\frac{1}{2}(H_0 - E)\phi^2 - \frac{1}{2} V \phi^2 - \frac{1}{2w^2} V^2 \right] \tag{2.27}$$

Here the benefit of choosing V to have a Gaussian distribution becomes clear, since the integral over V can now easily be performed. After integrating over V the expression becomes

$$\langle \mathcal{Z}_V(E) \rangle = \int_{-\infty}^{\infty} \frac{\mathrm{d}\phi}{\sqrt{2\pi}} \exp\left[-\frac{1}{2}(H_0 - E)\phi^2 + \frac{1}{8} w^2 \phi^4 \right]. \tag{2.28}$$

Since w^2 is positive, this integral will be divergent. It is possible however to make it convergent using analytic continuation, as discussed in the next section.

2.3.3 Analytic continuation

The majority of the analysis in this chapter comes from Chapter 39 of "Quantum Field Theory and Critical Phenomena" [11] by Zinn-Justin, repeated here for a better understanding of the problem.

Consider an integral on the form

$$I(g) = \frac{1}{\sqrt{2\pi}} \int \mathrm{d}x \exp\left[-\frac{1}{2}x^2 - \frac{1}{4}gx^4\right], \tag{2.29}$$

with $g > 0$. By the substitution $\phi \mapsto \phi\sqrt{H_0 - E}$, one sees that this (up to some factor) is equivalent to the expression for $\langle \mathcal{Z}_V(E) \rangle$ with $g = -\frac{w^2}{2(H_0-E)^2}$, as long as the energy is small enough so that $H_0 - E > 0$. For $g \gg 1$, the value of this integral will be dominated by the saddle point at the origin

$$I(g) = 1 + \mathcal{O}(g). \tag{2.30}$$

This integral only converges for $\mathrm{Re}g \geq 0$, but one can analytically continue $I(g)$ into the negative complex half plane $\mathrm{Re}g < 0$ by rotating the integration contour so that $\mathrm{Re}g\phi^4$ remains non-negative. In particular, for any g that is not on the negative real line one can pick a contour C such that $\arg\phi = -\frac{1}{4}\arg g$, ensuring that $\mathrm{Re}g\phi^4$ is positive. This gives rise to two different expressions for $I(g)$ depending on whether one rotated the contour clockwise or anticlockwise

$$I(-|g| + i0) \equiv \lim_{\epsilon\to 0} I(-|g| + i\epsilon) = \frac{1}{\sqrt{2\pi}} \int_{C_+} \mathrm{d}\phi \exp\left[-\frac{1}{2}\phi^2 - \frac{1}{4}g\phi^4\right], \tag{2.31}$$

$$I(-|g| - i0) \equiv \lim_{\epsilon\to 0} I(-|g| - i\epsilon) = \frac{1}{\sqrt{2\pi}} \int_{C_-} \mathrm{d}\phi \exp\left[-\frac{1}{2}\phi^2 - \frac{1}{4}g\phi^4\right], \tag{2.32}$$

with

$$C_+ : \ \arg\phi = -\frac{1}{4}\pi, \tag{2.33}$$

$$C_- : \ \arg\phi = \frac{1}{4}\pi. \tag{2.34}$$

These paths are visualized in Figure 2.1. Since $e^{i\pi/4} = \overline{e^{-i\pi/4}}$ the integral $I(-|g| + i0) = \overline{I(-|g| - i0)}$. In both cases the integral will still be dominated by the saddle point at the origin (which is of order 1) since the other saddle points to the equation give

$$\phi - |g|\phi^3 = 0 \implies \phi^2 = \frac{1}{|g|}, \tag{2.35}$$

and thus their contribution is of order $e^{-1/4|g|} \ll 1$ for $|g|$ small. Since the two integrals are conjugate, one can extract their imaginary part by taking their difference

$$2i\mathrm{Im}\ I(-|g|+i0) = I(-|g|+i0) - I(-|g|-i0) = \frac{1}{\sqrt{2\pi}} \int_{C_+ - C_-} \mathrm{d}\phi \exp\left[-\frac{1}{2}\phi^2 - \frac{1}{4}g\phi^4\right]. \tag{2.36}$$

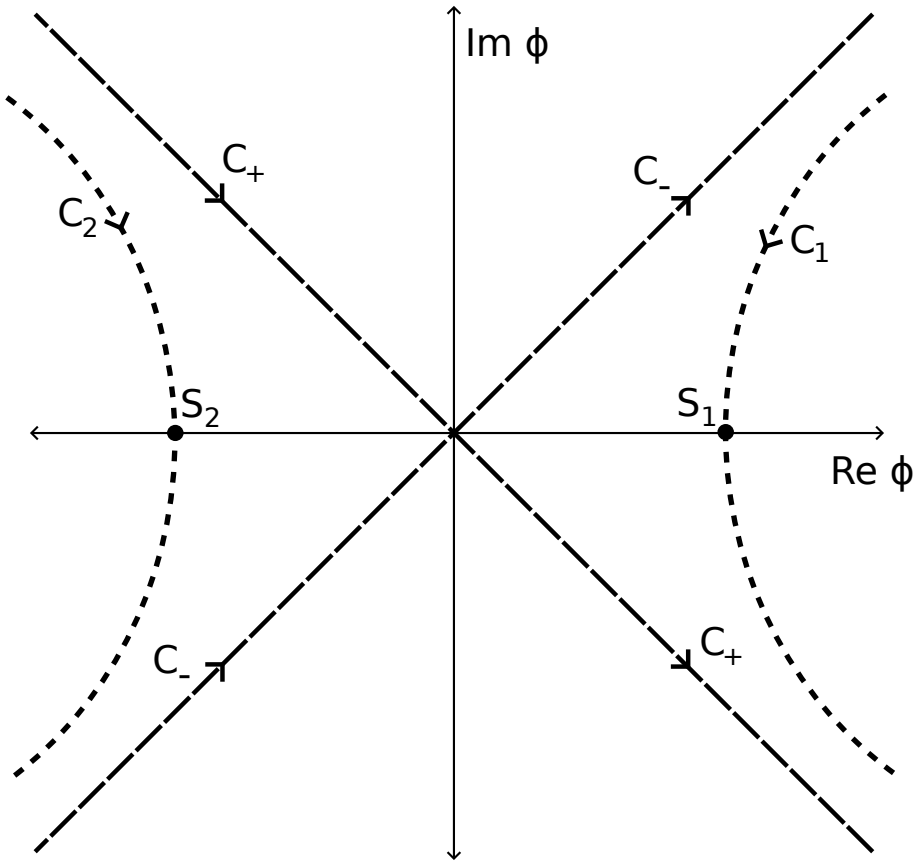

Figure 2.1: Integration contours in the analytic continuation. The contours $C_\pm$ correspond to the intervals $e^{\mp i\pi/4} \times (-\infty, \infty)$. In the path $C_2 - C_1$ the singularity at the origin is cancelled and can be deformed into the sum $C_1 + C_2$.

Since they both cross each other at the origin, the contributions at this point cancel out. One can thus deform the path $C_+ - C_-$ into the sum of two new paths C_1 and C_2, see Figure 2.1

The integral over $C_1 + C_2$ will be dominated by the contributions from the saddle points at $\phi = \pm\sqrt{1/|g|}$. Inserting this value into the integrand in equation 2.29 one sees tat the integrand at the saddle points is $e^{-\frac{1}{4|g|}}$, so Im $I(-|g|) \sim e^{-\frac{1}{4|g|}}$. Inserting the value for g in this equation gives $e^{-\frac{1}{4|g|}} = e^{-\frac{(H_0-E)^2}{2w^2}}$, which is the same exponential dependence as the average density of states (Eq. 2.18). Note that the contour C_- is precisely the integration contour needed to make the expression for $\langle \mathcal{Z}_V(E + i\epsilon)\rangle$ in Eq. 2.28 convergent for all values of V, which further motivates this procedure.

2.3.4 Average of n copies of the partition function

Just as with one copy, one can write the product of n copies of the partition function as a Gaussian integral as well

$$\begin{aligned}\mathcal{Z}_V^n(E) &= \int \frac{\mathrm{d}^n\phi}{(2\pi)^{n/2}} \prod_{j=1}^{n} \left(\exp\left[-\frac{1}{2}(H_0+V-E)\phi_j^2\right]\right) \\ &= \int \frac{\mathrm{d}^n\phi}{(2\pi)^{n/2}} \exp\left[-\frac{1}{2}(H_0+V-E)\sum_{j=1}^{n}\phi_j^2\right], \end{aligned} \tag{2.37}$$

where j labels the integration variable in the different integrals. Defining $\phi^2 \equiv \sum_{j=1}^{n}\phi_j^2$ and taking the average over all potentials gives us

$$\begin{aligned}\langle \mathcal{Z}_V^n(E)\rangle &= \int\int \frac{\mathrm{d}^n\phi}{(2\pi)^{n/2}} \int \mathrm{d}V \exp\left[-\frac{1}{2}(H_0-E)\phi^2 - \frac{1}{2}V\phi^2 - \frac{1}{2w^2}V^2\right] \\ &= \int\int \frac{\mathrm{d}^n\phi}{(2\pi)^{n/2}} \exp\left[-\frac{1}{2}(H_0-E)\phi^2 + \frac{1}{8}w^2\phi^4\right], \end{aligned} \tag{2.38}$$

where $\phi^4 \equiv (\phi^2)^2 = \left(\sum_{j=1}^{n}\phi_j^2\right)^2$. By the same argument as before, the imaginary part of this will be dominated by the saddle points at $|\phi| = \sqrt{2(H_0-E)^2/w^2}$, where $|\phi| = \sqrt{\phi^2}$. This time however, instead of having just two saddle points the saddle points form a $n-1$-sphere centered around the origin. This can be directly seen due to the fact that the integral is invariant rotations of the ϕ's.

To fully calculate this, one would need to first integrate over the angular part of the integral and then rotate the final contour. The exponentially decaying part however will still come from the saddle points and as in the case for the single copy, will have the value $\mathrm{Im}\,\langle \mathcal{Z}_V^n(E)\rangle \sim e^{-\frac{(H_0-E)^2}{2w^2}}$.

This exponential decay also survives into the full expression for the density of states. To see this, first write $\mathrm{Im}\,\langle \mathcal{Z}_V^n(E)\rangle = C_n(E)e^{-\frac{(H_0-E)^2}{2w^2}}$, where $C_n(E)$ is the non-exponential part of the density of states coming from evaluating the whole integral. Then, using this together with the replica trick gives

$$\begin{aligned}&\frac{\partial}{\partial E}\mathrm{Im}\,\langle \log \mathcal{Z}_V(E)\rangle = \frac{\partial}{\partial E}\mathrm{Im}\lim_{n\to 0}\frac{\langle \mathcal{Z}_V^n(E)\rangle - 1}{n} \\ &= \lim_{n\to 0}\frac{\partial}{\partial E}\mathrm{Im}\frac{\langle \mathcal{Z}_V^n(E)\rangle}{n} = \lim_{n\to 0}\frac{\partial}{\partial E}\frac{C_n(E)e^{-\frac{(H_0-E)^2}{2w^2}}}{n} \\ &= \lim_{n\to 0}\frac{\left(C_n'(E) - C_n(E)\frac{E-H_0}{w^2}\right)e^{-\frac{(H_0-E)^2}{2w^2}}}{n} \\ &= e^{-\frac{(H_0-E)^2}{2w^2}}\lim_{n\to 0}\frac{\left(C_n'(E) - C_n(E)\frac{E-H_0}{w^2}\right)}{n}. \end{aligned} \tag{2.39}$$

Although one can perform all the angular integrals and limits to get back the exact result for $\rho(E)$, in this thesis I am only interested in extracting the exponential

dependence. For the toy model the factor in front is simply a constant (Eq. 2.18) but for the real problem I am interested in this factor will in general be some power of $|E|$. This method can also be extended to models with more than 0 spatial dimensions, which I will discuss in the next section.

2.4 Average density of states for an electron in a random potential

As I have shown it is possible model the band tails originating from impurities by considering free electrons moving in a disorder potential. In this chapter I will calculate the tails using path integrals. At first I will assume that the particles have a parabolic dispersion, but at the end of the chapter I will generalize it to a more general dispersion relation.

2.4.1 Path integrals and random potentials

As I have noted multiple times the impurities in a solid can be modeled by a random potential, since the exact configuration of impurities inside a material caanot be known, and will thus effectively be random. Defining such a potential is however not quite straightforward. In the toy example in Section 2.3 the random potential was described by a single random number, which is straightforward to handle analytically.

To describe a continuous random potential inside a solid one needs to sample a random real number $V(\mathbf{x})$ at every point $\mathbf{x}$ in the solid. Effectively this means sampling an infinite-dimensional probability distribution, which is slightly trickier.

One way of handling this is to use path integrals. This implies that one first considers a discrete version of the problem, which can be expressed analytically, and then views the continuous case as a limit for finer and finer grids. To be concrete, let Λ be a square lattice over the volume with lattice parameter a_0. Instead of a continuous position $\mathbf{x}$ I now only consider the finite set of points on the grid $\mathbf{x}_i, i \in \Lambda$. At each point $\mathbf{x}_i$ of the lattice the potential $V(\mathbf{x}_i) \equiv V_i$ will be a random variable. In this way, one can reduce the potential from an infinite-dimensional random distribution to a finite-dimensional distribution.

I will furthermore assume that this potential is described by a Gaussian distribution. The main reason for this is that Gaussian functions are easy to handle analytically. In this thesis I will mainly use two simple identities. First, for any $n \times n$ symmetric and positive definite matrix A

$$\int \mathrm{d}^n v \exp\left[-\frac{1}{2}\mathbf{v}^T A \mathbf{v}\right] = \sqrt{2\pi \det A^{-1}}, \tag{2.40}$$

where $\mathbf{v} = (v_1, v_2, ..., v_n)^T$ is a vector and the integral goes over all of its components. The second identity (really a generalization of the first) which also holds for M

symmetric and positive definite is

$$\int \mathrm{d}^n v \exp\left[-\frac{1}{2}\mathbf{v}^T A\mathbf{v} + \mathbf{j}^T \cdot \mathbf{v}\right] = \sqrt{2\pi \det A^{-1}} e^{-\frac{1}{2}\mathbf{j}^T A^{-1}\mathbf{j}}. \tag{2.41}$$

These identities also make Gaussian distributions analytically simple. Consider an n-dimensional Gaussian distribution with mean $\boldsymbol{\mu}$ and covariance matrix M. The probability density will then simply be given by

$$p(v_1, v_2, ..., v_n) = \frac{1}{\sqrt{2\pi \det M}} \exp\left[-\frac{1}{2}(\mathbf{v} - \boldsymbol{\mu})^T M^{-1}(\mathbf{v} - \boldsymbol{\mu})\right], \tag{2.42}$$

with Eq. 2.40 ensuring that the overall probability is 1.

This makes it very easy to define Gaussian distributions with an arbitrary symmetric, positive definite covariance matrix M. For the potential, as discussed in Section 2.2 I set the mean to be 0, i.e $\langle V_i \rangle = 0, i \in \Lambda$. This means that the covariance has the simple form $\mathrm{cov}(V_i, V_j) \equiv M_{ij} = \langle V_i V_j \rangle$. When taking the continuous limit $a_0 \to 0$ this covariance will become symmetric function of the coordinates $M_{ij} \sim M(\mathbf{x}_i, \mathbf{x}_j) = M(\mathbf{x}_j, \mathbf{x}_i)$.

Assuming that the correlation of the potential between different points only depends on the distance between them allows a further simplification of the covariance $M(\mathbf{x}, \mathbf{y}) = M(\mathbf{x} - \mathbf{y})$, where $M(\mathbf{x})$ only depends of the length of $\mathbf{x}$. To simplify future calculations I will also split $M(\mathbf{x}) = w^2 C(\mathbf{x})$, where $w^2 \equiv \int \mathrm{d}^d x M(\mathbf{x})$ into a variance w^2 and a correlation function $C(\mathbf{x})$ with unit norm. This way I can independently quantify the strength of the random potential w^2 from the shape of the correlation function.

In this thesis I will assume that the random potential either has a Gaussian correlation

$$C(\mathbf{x}) = \frac{1}{(\pi\lambda_0^2)^{d/2}} e^{-\frac{|\mathbf{x}|^2}{\lambda_0^2}}, \tag{2.43}$$

or that it is completely uncorrelated

$$C(\mathbf{x}) = \delta(\mathbf{x}), \tag{2.44}$$

where λ_0 is the correlation length.

All in all one can summarize the random potential in the discrete case by

$$\langle V_i \rangle = 0 \tag{2.45}$$
$$\langle V_i V_j \rangle = M_{ij}, \tag{2.46}$$

and in the continuous case by

$$\langle V(\mathbf{x}) \rangle = 0 \tag{2.47}$$
$$\langle V(\mathbf{x}) V(\mathbf{y}) \rangle = w^2 C(\mathbf{x} - \mathbf{y}), \tag{2.48}$$

where I take the continuous case as the limit when the lattice spacing goes to zero $a_0 \to 0$.

Expressing the potential in this way makes it easy to average a potential dependent quantity Q_V over all lattice configurations. Writing the potential as a vector $\mathbf{V}$ with components V_i gives

$$Q = \langle Q_V \rangle = \frac{1}{\mathcal{N}_0} \int \mathcal{D}[V] \; Q_V \exp\left[-\frac{1}{2}\mathbf{V}^T M^{-1} \mathbf{V}\right], \tag{2.49}$$

where $\mathcal{D}[V] = \prod_{i\in\Lambda} dV_i$ and $\mathcal{N}_0 = \sqrt{2\pi \det M}$.

2.5 Integrating the density of states

In the continuous problem the energy levels of the system are given by the eigenvalues E_n^V of the Hamiltonian H^V. Here the superscript V indicates that both the Hamiltonian and its eigenvalues depend on the random potential. The Hamiltonian can naturally be split into two parts $H^V(\mathbf{x}) = H_0(\mathbf{x}) + V(\mathbf{x})$, where $H_0(\mathbf{x})$ is the kinetic part coming from the dispersion relation (and therefore independent of the disorder potential) and $V(\mathbf{x})$ is the potential part coming directly from the disorder potential. Assuming a parabolic dispersion relation this Hamiltonian will be the same as in Eq. 2.4, but no matter the exact dispersion relation the Hamiltonian will be an operator acting on wavefunctions $\psi(\mathbf{x})$ in the solid.

When discretizing the problem however the wavefunctions $\psi(\mathbf{x}_i)$ will only be defined on the points $\mathbf{x}_i$ that are part of the lattice Λ. Since this is a finite number of points, the resulting wavefunctions can be described by vectors $\boldsymbol{\psi}$ with components $\psi(\mathbf{x}_i)$. The discretized Hamiltonian will thus be a matrix acting on the wavefunctions $\boldsymbol{\psi}$. Importantly this means that the discrete system only has a finite number of eigenvalues. Thus one can use the definition in Eq. 2.6 to write the density of states as

$$\rho_V(E) = \frac{1}{V_d} \sum_n \delta(E - E_n^V), \tag{2.50}$$

where V_d is the volume of the solid and E_n^V are the eigenvalues of the Hamiltonian. Here, the superscript and subscript V indicate that the quantities depend on the configuration depend on the random potential. Averaging over all configurations of the random potential gives the disorder averaged density of states as

$$\rho(E) \equiv \left\langle \frac{1}{V_d} \sum_n \delta(E - E_n^V) \right\rangle = \frac{1}{\mathcal{N}_0} \int \mathcal{D}[V] \; \exp\left[-\frac{1}{2}\mathbf{V}^T M_{ij}^{-1} \mathbf{V}\right] \times \frac{1}{V_d} \sum_n \delta(E - E_n^V), \tag{2.51}$$

with $\mathcal{D}[V] = \prod_{i\in\Lambda} \mathrm{d}V_i$.

This expression looks similar to the one in Eq. 2.17, but now there is no nice relationship between the configuration of the disorder potential and the energy levels. To handle with this one can proceed similarly to the second method described in Section 2.3. Again, I start by introducing the partition function

$$\mathcal{Z}_V(E) = \left[\prod_n (E_n^V - E)\right]^{-1/2} = \left[\det\{H^V - E\}\right]^{-1/2}. \tag{2.52}$$

Here the second equality holds since the discrete Hamiltonian is a matrix. Then note that

$$2\frac{\partial}{\partial E}\log \mathcal{Z}_V(E) = 2\frac{\partial}{\partial E}\log\left[\prod_n (E_n^V - E)\right]^{-1/2} \\ = -\frac{\partial}{\partial E}\sum_n \log\{E_n^V - E\} = -\sum_n \frac{1}{E - E_n^V}. \tag{2.53}$$

Using the definition of the delta function in Eq. 2.20 gives

$$\rho_V(E) = \frac{1}{V_d}\sum_n \delta(E - E_n^V) = \lim_{\epsilon\to 0}\frac{2}{\pi V_d}\mathrm{Im}\frac{\partial}{\partial E}\log \mathcal{Z}_V(E + i\epsilon) \tag{2.54}$$

The disorder averaged density of states can thus be written as

$$\rho(E) = \langle \rho_V(E)\rangle = \lim_{\epsilon\to 0}\frac{2}{\pi V_d}\mathrm{Im}\frac{\partial}{\partial E}\langle \log \mathcal{Z}_V(E + i\epsilon)\rangle. \tag{2.55}$$

2.5.1 Quenched average path integral

The quantity $\langle \log \mathcal{Z}_V\rangle$ can just as in section 2.3 be calculated using the replica trick 2.24. This means that I now have to find an expression for $\mathcal{Z}_V^n(E)$

In Section 2.3, the partition function could be expressed using a one-dimensional Gaussian integral, and similarly in this case one can write it as a multidimensional Gaussian integral. To do this I introduce an auxilliary real field $\phi(\mathbf{x})$ on the volume. Just as with the potential and the wave functions, I discretize it on the lattice Λ, and write it as a finite dimensional vector $\boldsymbol{\phi}$, with components $\phi(\mathbf{x}_i)$. Using the definition of the partition function 2.52 and the analytical expression for a Gaussian integral 2.40 one can write the partition function as

$$\mathcal{Z}_V(E) = \int \mathcal{D}[\phi]\exp\left[-\frac{1}{2}\boldsymbol{\phi}^T H\boldsymbol{\phi}\right], \tag{2.56}$$

with $\mathcal{D}[\phi] = \prod_{i\in\Lambda} \mathrm{d}\phi(\mathbf{x}_i)/\sqrt{2\pi}$.

The average of one single partition function is thus given by

$$\langle \mathcal{Z}_V\rangle = \frac{1}{\mathcal{N}_0}\int \mathcal{D}[V]\mathcal{D}[\phi]\exp\left[-\frac{1}{2}\mathbf{V}^T M^{-1}\mathbf{V} - \frac{1}{2}\boldsymbol{\phi}^T(H_0 + V - E)\boldsymbol{\phi}\right]. \tag{2.57}$$

Note here that the potential enters this expression in two different ways. First it enters as a vector of the lattice points $\mathbf{V}$ from the probability density function, but it also enters as a part of the Hamiltonian. This second V must thus be a matrix. Since potentials are diagonal in the position basis and $\boldsymbol{\phi}$ is also defined in the position basis, one can write the components of V acting on $\boldsymbol{\phi}$ as $V_{ij} = V_i\delta_{ij} = V(\mathbf{x}_i)\delta_{ij}$. Therefore

$$\boldsymbol{\phi}^T V\boldsymbol{\phi} = \phi(\mathbf{x}_i)V_i\delta_{ij}\phi(\mathbf{x}_j) = \sum_{i\in\Lambda} V_i\phi^2(\mathbf{x}_i) \equiv \boldsymbol{\Phi}\cdot\mathbf{V}, \tag{2.58}$$

where $\mathbf{\Phi}$ is a vector with components $\phi^2(\mathbf{x}_i)$. Performing the integral over V thus gives

$$\frac{1}{\mathcal{N}_0}\int \mathcal{D}[V]\exp\left[-\frac{1}{2}\mathbf{V}^T M^{-1}\mathbf{V}-\frac{1}{2}\mathbf{\Phi}\cdot\mathbf{V}\right]=\exp\left[\frac{1}{8}\mathbf{\Phi}^T M\mathbf{\Phi}\right] \tag{2.59}$$

Thus

$$\langle\mathcal{Z}_V\rangle=\int\mathcal{D}[\phi]\exp\left[-\frac{1}{2}\boldsymbol{\phi}^T(H_0-E)\boldsymbol{\phi}+\frac{1}{8}\mathbf{\Phi}^T M\mathbf{\Phi}\right]. \tag{2.60}$$

For n copies of the partition function I introduce n different fields ϕ_j, with $j=1,...,n$ labeling the different copies. The discretized vectors will therefore also need the same label, so one gets the vectors $\boldsymbol{\phi}_j$ with components $\phi_j(\mathbf{x}_i)$, with j labeling the different copies and i labeling the point on the lattice. The average will then be

$$\langle\mathcal{Z}_V\rangle=\frac{1}{\mathcal{N}_0}\int\mathcal{D}[V]\mathcal{D}[\phi]\exp\left[-\frac{1}{2}\mathbf{V}^T M^{-1}\mathbf{V}-\frac{1}{2}\sum_{j=1}^{n}\boldsymbol{\phi}_j^T(H_0+V-E)\boldsymbol{\phi}_j\right], \tag{2.61}$$

with $\mathcal{D}[\phi]=\prod_{i\in\Lambda}\prod_{j=1}^{n}\frac{\mathrm{d}\phi_j(\mathbf{x}_i)}{\sqrt{2\pi}}$. Following the same argument as for a single copy that the matrix V is diagonal in the position basis gives

$$\sum_{j=1}^{n}\boldsymbol{\phi}_j V\boldsymbol{\phi}_j=\sum_{j=1}^{n}\mathbf{V}\cdot\mathbf{\Phi}_j=\mathbf{V}\cdot\left(\sum_{j=1}^{n}\mathbf{\Phi}_j\right), \tag{2.62}$$

with $\mathbf{\Phi}_j$ having components $\phi_j^2(\mathbf{x}_i)$. Performing the integral over V then gives us

$$\frac{1}{\mathcal{N}_0}\int\mathcal{D}[V]\exp\left[-\frac{1}{2}\mathbf{V}^T M^{-1}\mathbf{V}-\frac{1}{2}\left(\sum_{j=1}^{n}\mathbf{\Phi}_j\right)\cdot\mathbf{V}\right]=\exp\left[\frac{1}{8}\left(\sum_{j=1}^{n}\mathbf{\Phi}_j\right)^T M\left(\sum_{j=1}^{n}\mathbf{\Phi}_j\right)\right], \tag{2.63}$$

and thus the average of n copies of the partition function is given by

$$\langle\mathcal{Z}_V^n\rangle=\int\mathcal{D}[\phi]\exp\left[-\frac{1}{2}\sum_{j=1}^{n}\boldsymbol{\phi}_j^T(H_0-E)\boldsymbol{\phi}_j+\frac{1}{8}\left(\sum_{j=1}^{n}\mathbf{\Phi}_j\right)^T M\left(\sum_{j=1}^{n}\mathbf{\Phi}_j\right)\right]. \tag{2.64}$$

Now, in the continuous limit the sum

$$\sum_{i\in\Lambda}a_0^d f(\mathbf{x}_i)\approx\int\mathrm{d}^d x\ f(\mathbf{x}) \tag{2.65}$$

In the first term in the exponent each j thus becomes

$$\begin{aligned}\boldsymbol{\phi}_j^T(H_0-E)\boldsymbol{\phi}_j&=\frac{1}{a_0^d}\sum_{i,k\in\Lambda}a_0^d\phi_j(\mathbf{x}_i)(H_0-E)_{ik}\phi_j(\mathbf{x}_k)\\&\approx\frac{1}{a_0^d}\int\mathrm{d}^d x\ \phi_j(\mathbf{x})\left(-\frac{\hbar^2}{2m}\nabla^2-E\right)\phi_j(\mathbf{x}).\end{aligned} \tag{2.66}$$

In the continuum limit then it is appropriate to rescale $\phi(\mathbf{x}) \mapsto a_0^{d/2}\phi(\mathbf{x})$. This also then requires the shift

$$\mathcal{D}[\phi] \mapsto \prod_{j=1}^{n}\prod_{i\in\Lambda}\sqrt{\frac{a_0^d}{2\pi}}\mathrm{d}\phi_j(\mathbf{x}_i) \tag{2.67}$$

Using this the second term in the exponent becomes

$$\begin{aligned}\left(\sum_{j=1}^{n}\mathbf{\Phi}_j\right)^T M\left(\sum_{j=1}^{n}\mathbf{\Phi}_j\right) &\mapsto a_0^{2d}\left(\sum_{j=1}^{n}\mathbf{\Phi}_j\right)^T M\left(\sum_{j=1}^{n}\mathbf{\Phi}_j\right)\\ &= \sum_{k,l\in\Lambda} a_0^{2d}\left(\sum_{j=1}^{n}\Phi_j(\mathbf{x}_k)\right)M_{kl}\left(\sum_{j=1}^{n}\Phi_j(\mathbf{x}_l)\right)\\ &= \sum_{k,l\in\Lambda} a_0^{2d}\left(\sum_{j=1}^{n}\phi_j(\mathbf{x}_k)^2\right)M_{kl}\left(\sum_{j=1}^{n}\phi_j(\mathbf{x}_l)^2\right)\\ &\approx \int \mathrm{d}^dx\mathrm{d}^dy\ \left(\sum_{j=1}^{n}\phi_j^2(\mathbf{x})\right)w^2C(\mathbf{x}-\mathbf{y})\left(\sum_{j=1}^{n}\phi_j^2(\mathbf{y})\right).\end{aligned} \tag{2.68}$$

In the continuum limit then the partition function becomes

$$\begin{aligned}\langle\mathcal{Z}_V^n\rangle = \int\mathcal{D}[\phi]\exp\Bigg[-\frac{1}{2}\int\mathrm{d}^dx\ \sum_{j=1}^{n}\phi_j(\mathbf{x})\left(-\frac{\hbar^2}{2m}\nabla^2-E\right)\phi_j(\mathbf{x})\\ +\frac{w^2}{8}\int\mathrm{d}^dx\mathrm{d}^dy\ \phi^2(\mathbf{x})C(\mathbf{x}-\mathbf{y})\phi^2(\mathbf{y})\Bigg],\end{aligned} \tag{2.69}$$

where $\phi^2(\mathbf{x}) \equiv \sum_{j=1}^{n}\phi_j^2(\mathbf{x})$.

Before moving on it is convenient to again rescale ϕ, as well as rescaling the length in order to make the action unitless. As I will show see this makes it easy to separate out most dimensional quantities in the problem and gives an action that effectively depends on just a few parameters.

To start, I rescale the positions $\mathbf{x} \mapsto l\mathbf{x} = \sqrt{\hbar^2/2m|E|}\mathbf{x}$ so that both terms in the single integral have the same coefficients

$$\begin{aligned}&\sum_{j=1}^{n}\phi_j(\mathbf{x})\phi(\mathbf{x})\left(-\frac{\hbar^2}{2m}\nabla^2-E\right)\phi_j(\mathbf{x})\\ &\mapsto \sum_{j=1}^{n}\phi_j(\mathbf{x})\left(-|E|\nabla^2+|E|\right)\phi_j(\mathbf{x}).\end{aligned} \tag{2.70}$$

This rescaling also multiplies the whole integral by a factor of $l^d = (\hbar^2/2m|E|)^{d/2}$ from the integral measure d^dx. The length rescaling also affects the double integral which is rescaled by a factor l^{2d}. One can factor out one copy of l^d to have the same factor as the single integral, but the second factor of l^d will effectively rescale the correlation length.

Before calculating this however, to get the same factor for both integrals I also rescale the fields ϕ_j themselves to $\phi \mapsto (2|E|/w^2)^{1/2}\phi$. The total effect of this on the first integral is

$$\begin{aligned} &-\frac{1}{2}\int \mathrm{d}^d x\ \phi(\mathbf{x})\left(-\frac{\hbar^2}{2m}\nabla^2 - E\right)\phi(\mathbf{x}) \\ &\mapsto -\frac{2|E|^2}{w^2}\left(\frac{\hbar^2}{2m|E|}\right)^{d/2}\int \mathrm{d}^d x\ \sum_{j=1}^{n}\phi(\mathbf{x})\left(-\frac{1}{2}\nabla^2 + \frac{1}{2}\right)\phi(\mathbf{x}). \end{aligned} \tag{2.71}$$

For the second term, exactly how the correlation length gets modified depends on whether or not $C(\mathbf{x})$ is a Gaussian or a delta function. If $C(\mathbf{x})$ is a delta function the second term becomes

$$\begin{aligned} &\frac{w^2}{8}\int \mathrm{d}^d x \mathrm{d}^d y\ \phi^2(\mathbf{x})C(\mathbf{x}-\mathbf{y})\phi^2(\mathbf{y}) = \frac{w^2}{8}\int \mathrm{d}^d x\ \phi^4(\mathbf{x}) \\ &\mapsto \frac{2|E|^2}{w^2}\left(\frac{\hbar^2}{2m|E|}\right)^{d/2}\int \mathrm{d}^d x\ \frac{1}{4}\phi^4(\mathbf{x}), \end{aligned} \tag{2.72}$$

where $\phi^4(\mathbf{x}) \equiv (\phi^2(\mathbf{x}))^2$. If instead $C(\mathbf{x})$ is Gaussian the second term becomes

$$\begin{aligned} &\frac{w^2}{8}\int \mathrm{d}^d x \mathrm{d}^d y\ \phi^2(\mathbf{x})C(\mathbf{x}-\mathbf{y})\phi^2(\mathbf{y}) = \frac{w^2}{8}\int \mathrm{d}^d x \mathrm{d}^d y\ \phi^2(\mathbf{x})\frac{e^{-(\mathbf{x}-\mathbf{y})^2/\lambda_0^2}}{(\pi\lambda_0^2)^{d/2}}\phi^2(\mathbf{y}) \\ &\mapsto \frac{2|E|^2}{w^2}\left(\frac{\hbar^2}{2m|E|}\right)^{d/2}\int \mathrm{d}^d x \mathrm{d}^d y\ \frac{1}{4}\phi^2(\mathbf{x})\frac{l^d}{(\pi\lambda_0^2)^{d/2}}e^{-(l\mathbf{x}-l\mathbf{y})^2/\lambda_0^2}\phi^2(\mathbf{y}) \\ &= \frac{2|E|^2}{w^2}\left(\frac{\hbar^2}{2m|E|}\right)^{d/2}\int \mathrm{d}^d x \mathrm{d}^d y\ \frac{1}{4}\phi^2(\mathbf{x})l^d C\left(l(\mathbf{x}-\mathbf{y})\right)\phi^2(\mathbf{y}), \end{aligned} \tag{2.73}$$

with $l = \sqrt{\hbar^2/2m|E|}$ as before. These two cases for the correlation can be summarized by explicitly writing out the dependence on the correlation length. Since the delta function can be seen as a limit of the Gaussian when the correlation length goes to zero, it can be written as

$$C_r(\mathbf{x}) = \frac{1}{(\pi r^2)^{d/2}}e^{-\mathbf{x}^2/r^2} \text{ for } r > 0, \tag{2.74}$$

$$C_0 = \lim_{r\to 0} C_r(\mathbf{x}) = \delta(\mathbf{x}), \tag{2.75}$$

where r is the width of the Gaussian. Letting $\lambda \equiv \lambda_0/l$ Gaussian correlations get modified as

$$C_{\lambda_0}(\mathbf{x}) \mapsto l^d C_{\lambda_0}(l\mathbf{x}) = \sqrt{\frac{l^d}{2\pi\lambda_0^d}}e^{-\left(\frac{l}{\lambda_0}(\mathbf{x}-\mathbf{y})\right)^2} = C_\lambda(\mathbf{x}), \tag{2.76}$$

where $\lambda \equiv \lambda_0/l$. In both cases then, when normalizing the variables the correlation length effectively gets modified by a factor of $1/l$. For the delta function with $\lambda_0 = 0$

this has no effect, but it matters for the Gaussian correlation. Then combining these results gives

$$\begin{aligned}&\frac{w^2}{8}\int \mathrm{d}^d x \mathrm{d}^d y\ \phi^2(\mathbf{x}) C_{\lambda_0}(\mathbf{x}-\mathbf{y})\phi^2(\mathbf{y})\\ &\mapsto \frac{2|E|^2}{w^2}\left(\frac{\hbar^2}{2m|E|}\right)^{d/2}\int \mathrm{d}^d x \mathrm{d}^d y\ \frac{1}{4}\phi^2(\mathbf{x}) C_{\lambda}(\mathbf{x}-\mathbf{y})\phi^2(\mathbf{y}),\end{aligned} \tag{2.77}$$

where $\lambda \equiv \lambda_0/\sqrt{\hbar^2/2m|E|}$. Combining everything one arrives at the compact equation

$$\langle \mathcal{Z}_V^n \rangle = \int \mathcal{D}[\phi] e^{-gS[\phi]}, \tag{2.78}$$

with

$$\mathcal{D}[\phi] \equiv \prod_{j=1}^{n}\prod_{i\in\Lambda}\sqrt{\frac{2|E|a_0^d}{2\pi w^2}}\mathrm{d}\phi_j(\mathbf{x}_i), \tag{2.79}$$

$$g \equiv \frac{2|E|^2}{w^2}\left(\frac{\hbar^2}{2m|E|}\right)^{d/2}, \tag{2.80}$$

$$S[\phi] \equiv \int \mathrm{d}^d x\ \sum_{j=1}^{n}\phi_j(\mathbf{x})\left(-\frac{1}{2}\nabla^2+\frac{1}{2}\right)\phi_j(\mathbf{x}) - \int \mathrm{d}^d x \mathrm{d}^d y\ \frac{1}{4}\phi^2(\mathbf{x}) C_{\lambda}(\mathbf{x}-\mathbf{y})\phi^2(\mathbf{y}), \tag{2.81}$$

$$\lambda \equiv \lambda_0\sqrt{\frac{2m|E|}{\hbar^2}}. \tag{2.82}$$

In total, the average of n copies of the partition function can be written as a path integral over n replica fields $\phi_j(\mathbf{x})$ over the effective action given by 2.81. Interestingly one can also interpret this as the action for a set of n interacting bosonic quantum fields. In some sense then the introduction of a disorder potential causes an effective interaction between the electrons.

2.5.2 Evaluating the path integral

Just as for the toy model, the imaginary part of the partition function will be dominated by the non-trivial saddle points, in this context called instanton solutions, which also give rise to the exponentially decaying part of the density of states. The instanton solutions are in turn given as the extrema of the action $S[\phi]$, that is the paths such that $\delta S[\phi] = 0$. This variation is straightforward to evaluate using the fact that

$$\frac{\delta}{\delta\phi_k(\mathbf{x})}\phi_j(\mathbf{y}) = \delta_{kj}\delta(\mathbf{x}-\mathbf{y}). \tag{2.83}$$

Starting from the first term of the action in Eq. 2.81 gives

$$\begin{aligned}&\frac{\delta}{\delta\phi_k(\mathbf{x})}\left(\int \mathrm{d}^d y\ \sum_{j=1}^{n}\phi_j(\mathbf{y})\left(-\frac{1}{2}\nabla_{\mathbf{y}}^2+\frac{1}{2}\right)\phi_j(\mathbf{y})\right)\\ &= \int \mathrm{d}^d y\ \left\{\delta(\mathbf{x}-\mathbf{y})\left(-\frac{1}{2}\nabla_{\mathbf{y}}^2+\frac{1}{2}\right)\phi_k(\mathbf{y}) + \phi_k(\mathbf{y})\left(-\frac{1}{2}\nabla_{\mathbf{y}}^2+\frac{1}{2}\right)\delta(\mathbf{x}-\mathbf{y})\right\}.\end{aligned} \tag{2.84}$$

Now, note that

$$\int \mathrm{d}^d y \;\; f(\mathbf{y})\nabla^2_{\mathbf{y}}\delta(\mathbf{x}-\mathbf{y}) = (-1)^2 \int \mathrm{d}^d y \;\; \delta(\mathbf{x}-\mathbf{y})\nabla^2_{\mathbf{y}} f(\mathbf{y}) = \int \mathrm{d}^d y \;\; \delta(\mathbf{x}-\mathbf{y})\nabla^2_{\mathbf{y}} f(\mathbf{y}), \tag{2.85}$$

since all surface terms containing $\delta(\mathbf{x}-\mathbf{y})$ and $\nabla_{\mathbf{y}}\delta(\mathbf{x}-\mathbf{y})$ must vanish. Thus

$$\frac{\delta}{\delta\phi_k(\mathbf{x})}\left(\int \mathrm{d}^d y \;\; \sum_{j=1}^{n} \phi_j(\mathbf{y})\left(-\frac{1}{2}\nabla^2_{\mathbf{y}} + \frac{1}{2}\right)\phi_j(\mathbf{y})\right) = \tag{2.86}$$

$$\int \mathrm{d}^d y \;\; \delta(\mathbf{x}-\mathbf{y})\left(-\frac{1}{2}\nabla^2_{\mathbf{y}} + \frac{1}{2}\right)\phi_k(\mathbf{y}) = \left(-\nabla^2 + 1\right)\phi_k(\mathbf{x}). \tag{2.87}$$

For the second term in Eq. 2.81, note that

$$\frac{\delta}{\delta\phi_k(\mathbf{x})}\left(\sum_{j=1}^{n}\phi^2(\mathbf{y})\right) = 2\delta(\mathbf{x}-\mathbf{y})\phi_k(\mathbf{y}). \tag{2.88}$$

The variation of the second term is thus

$$\begin{aligned}
&\frac{\delta}{\delta\phi_k(\mathbf{x})}\left(\int \mathrm{d}^d y \mathrm{d}^d z \;\; \frac{1}{4}\phi^2(\mathbf{y})C_\lambda(\mathbf{y}-\mathbf{z})\phi^2(\mathbf{z})\right) \\
&= \frac{1}{4}\int \mathrm{d}^d y \mathrm{d}^d z \;\; \left(2\delta(\mathbf{x}-\mathbf{y})\phi_k(\mathbf{y})C_\lambda(\mathbf{y}-\mathbf{z})\phi^2(\mathbf{z}) + \phi^2(\mathbf{y})C_\lambda(\mathbf{y}-\mathbf{z})\cdot 2\delta(\mathbf{x}-\mathbf{z})\phi_k(\mathbf{z})\right) \\
&= \phi_k(\mathbf{x})\int \mathrm{d}^d y \;\; \phi^2(\mathbf{y})C_\lambda(\mathbf{x}-\mathbf{y}),
\end{aligned} \tag{2.89}$$

since y, z are interchangeable in the integrals. Combining these gives the conditions

$$0 = \frac{\delta S[\phi]}{\delta\phi_k(\mathbf{x})} = \left(-\nabla^2 + 1\right)\phi_k(\mathbf{x}) - \phi_k(\mathbf{x})\int \mathrm{d}^d y \;\; \phi^2(\mathbf{y})C_\lambda(\mathbf{x}-\mathbf{y}). \tag{2.90}$$

Note that this equation is invariant under rotations in replica space. To see this, let $\vec{\phi}(\mathbf{x}) = (\phi_1(\mathbf{x}), \phi_2(\mathbf{x}), ..., \phi_n(\mathbf{x}))^T$ Then $\phi^2 = \sum_{j=1}^{n}\phi_j^2(\mathbf{x}) = \vec{\phi}(\mathbf{x})^2$ and one can compactly write Eq. 2.90 as

$$\left(-\nabla^2 - 1 - \int \mathrm{d}^d y \;\; \vec{\phi}^2(\mathbf{y})C_\lambda(\mathbf{x}-\mathbf{y})\right)\vec{\phi}(\mathbf{x}) = 0. \tag{2.91}$$

Now let O be an n-dimensional orthogonal matrix through which one can define a new set of rotated fields

$$\phi'_j(\mathbf{x}) = \sum_{k=1}^{n} O_{jk}\phi_k(\mathbf{x}) \implies \vec{\phi}'(\mathbf{x}) = O\vec{\phi}(\mathbf{x}) \implies \vec{\phi}(\mathbf{x}) = O^T\vec{\phi}'(\mathbf{x}). \tag{2.92}$$

Since orthogonal matrices conserve the length of vectors $\phi^2 = \vec{\phi}(\mathbf{x})^2 = \vec{\phi}'(\mathbf{x})^2$. Eq. 2.91 can thus be written as

$$\begin{aligned}
&\left(-\nabla^2 - 1 - \int \mathrm{d}^d y \;\; \vec{\phi}'^2(\mathbf{y})C_\lambda(\mathbf{x}-\mathbf{y})\right)O^T\vec{\phi}'(\mathbf{x}) = 0 \\
&\implies \left(-\nabla^2 - 1 - \int \mathrm{d}^d y \;\; \vec{\phi}'^2(\mathbf{y})C_\lambda(\mathbf{x}-\mathbf{y})\right)\vec{\phi}'(\mathbf{x}) = 0
\end{aligned} \tag{2.93}$$

Where $\hat{n}$ is a unit vector . This means that any solution must be of the form $\vec{\phi}^\star(\mathbf{x}) = \hat{n} f^\star(\mathbf{x})$, where $f^\star(\mathbf{x})$ satisfies

$$\nabla^2 f^\star(\mathbf{x}) = f^\star(\mathbf{x}) - f^\star(\mathbf{x}) \int \mathrm{d}^d y \ (f^\star)^2(\mathbf{y}) C_\lambda(\mathbf{x}-\mathbf{y}). \tag{2.94}$$

Inserting this back into the action gives for instanton solutions $f^\star$

$$S[f^\star] = \frac{1}{4} \int \mathrm{d}^d x \mathrm{d}^d y \ f^{\star 2}(\mathbf{x}) C_\lambda(\mathbf{x}-\mathbf{y}) f^{\star 2}(\mathbf{y}) \tag{2.95}$$

From this action one also get a boundary condition for the instanton solution, namely that the instanton solution must go to zero at infinity, since the action would otherwise be infinite. To see this, suppose for example that the instanton solution were some constant $f^\star(\mathbf{x}) \equiv A$. Then, since $C_\lambda(\mathbf{x})$ is defined so that its integral equals 1, the action for this solution will be

$$S[f^\star] = \frac{1}{4} \int \mathrm{d}^d x \mathrm{d}^d y \ A^2 C_\lambda(\mathbf{x}-\mathbf{y}) A^2 = \frac{A^4}{4} \int \mathrm{d}^d x = \infty. \tag{2.96}$$

All in all the tails in the density of states are proportional to

$$\rho(E) \propto e^{-gS[f^\star]}, \tag{2.97}$$

where g is given by Eq. 2.80, $S[f^\star]$ is given by Eq. 2.95 and $f^\star(\mathbf{x})$ satisfies Eq. 2.94.

2.6 Instanton equation for different dispersion relations

The discussion in the previous section was restricted to parabolic dispersion relations. In this section, I will show how one can extend the calculation of the density of states to more general dispersion relations. In the case of the free particle Hamiltonian 2.3 I showed that it had a parabolic dispersion by looking at the energy spectrum but there is another way of calculating this. The dispersion relation is namely the Fourier transform of the kinetic term. In the context of the Schrödinger equation this can easily be seen. The Fourier transform of a function $f(\mathbf{x})$ is defined through

$$\mathcal{F}\{f\}(\mathbf{k}) = \hat{f}(\mathbf{k}) = \int \mathrm{d}^d x f(\mathbf{x}) e^{-i\mathbf{k}\cdot\mathbf{x}}. \tag{2.98}$$

Using the identity $\mathcal{F}\{\nabla^2 f(\mathbf{x})\}(\mathbf{k}) = -|\mathbf{k}|^2 \hat{f}(\mathbf{k})$ the Fourier transform of the free Schrödinger equation can be calculated

$$\mathcal{F}\{H(\mathbf{x})\psi(\mathbf{x})\} = \mathcal{F}\left\{-\frac{\hbar^2}{2m}\nabla^2\psi(\mathbf{x})\right\} = \frac{\hbar^2|\mathbf{k}|^2}{2m}\hat{\psi}(\mathbf{k}) = \mathcal{E}_{\text{free}}(\mathbf{k})\hat{\psi}(\mathbf{k}). \tag{2.99}$$

Extending this to arbitrary dispersion relations $\mathcal{E}(\mathbf{k})$ gives the kinetic term as

$$H_0(\mathbf{x})\psi(\mathbf{x}) = \mathcal{F}^{-1}\left\{\mathcal{E}(\mathbf{k})\hat{\psi}(\mathbf{k})\right\}, \tag{2.100}$$

where $\mathcal{F}^{-1}$ denotes the inverse Fourier transform. In principle with this method there are three restrictions on the $\mathcal{E}(\mathbf{k})$. First, since the dispersion relation gives to energy of the states in the band, it must be a real number. Second, since $\mathcal{E}(\mathbf{k})$ approximates the band structure at the bottom of a conduction band one expects that it goes to infinity when $|\mathbf{k}|$ goes to infinity. The third condition has to do with how the path integral was defined.

Remember that the fields I integrate over in the path integral are real fields $\phi(\mathbf{x})$. For this formulation to make sense I thus also require $H\phi(\mathbf{x})$ to be real. The potential part corresponds to a real number, so this condition is automatically fullfilled. For the kinetic part, this requires that $\mathcal{F}^{-1}\left\{\mathcal{E}(\mathbf{k})\hat{\phi}(\mathbf{k})\right\}$ be real when $\phi(\mathbf{x})$ is real.

Although the other two restrictions were more general in order for the dispersion relation to make sense, this third requirement seems to be more of an artefact of this particular method, since there is in principle nothing that prevents bands which break this. One way to possibly analyze dispersions which break this condition is to define the partition function in terms of a path integral over complex fields ϕ instead of the real fields I have been using, but this is not something I will do in my thesis.

The correct condition for the third requirement is to take $\mathcal{E}(\mathbf{k}) = \mathcal{E}(-\mathbf{k})$. To see this, note first that one can express any function $\phi(\mathbf{x})$ in terms of its Fourier transform by.

$$\phi(\mathbf{x}) = \frac{1}{(2\pi)^d}\int \mathrm{d}^d k \hat{\phi}(\mathbf{k}) e^{i\mathbf{k}\cdot\mathbf{x}}. \tag{2.101}$$

If $\phi(\mathbf{x})$ is real, then taking the complex conjugate of both sides of the equation yields

$$\begin{aligned}&\frac{1}{(2\pi)^d}\int \mathrm{d}^d k \hat{\phi}(\mathbf{k}) e^{i\mathbf{k}\cdot\mathbf{x}} = \frac{1}{(2\pi)^d}\int \mathrm{d}^d k \hat{\phi}^*(\mathbf{k}) e^{-i\mathbf{k}\cdot\mathbf{x}} = \frac{1}{(2\pi)^d}\int \mathrm{d}^d k \hat{\phi}^*(-\mathbf{k}) e^{i\mathbf{k}\cdot\mathbf{x}} \\ &\implies \hat{\phi}(\mathbf{k}) = \hat{\phi}^*(-\mathbf{k}),\end{aligned} \tag{2.102}$$

where $*$ indicates complex conjugation. Requiring that $\mathcal{F}^{-1}\left\{\mathcal{E}(\mathbf{k})\hat{\phi}(\mathbf{k})\right\}$ is real then means that

$$\begin{aligned}&\frac{1}{(2\pi)^d}\int \mathrm{d}^d k \mathcal{E}(\mathbf{k})\hat{\phi}(\mathbf{k}) e^{i\mathbf{k}\cdot\mathbf{x}} = \frac{1}{(2\pi)^d}\int \mathrm{d}^d k \mathcal{E}(\mathbf{k})\hat{\phi}^*(\mathbf{k}) e^{-i\mathbf{k}\cdot\mathbf{x}} = \frac{1}{(2\pi)^d}\int \mathrm{d}^d k \mathcal{E}(-\mathbf{k})\hat{\phi}^*(-\mathbf{k}) e^{i\mathbf{k}\cdot\mathbf{x}} \\ &= \frac{1}{(2\pi)^d}\int \mathrm{d}^d k \mathcal{E}(-\mathbf{k})\hat{\phi}(\mathbf{k}) e^{i\mathbf{k}\cdot\mathbf{x}},\end{aligned} \tag{2.103}$$

thus requiring $\mathcal{E}(\mathbf{k}) = \mathcal{E}(-\mathbf{k})$.

With these conditions on $\mathcal{E}(\mathbf{k})$ one can calculate the average density of states by repeating the exact same steps as in the parabolic case. This time I arrive at the following expression for the average of n copies of the partition function (compare with Eq. 2.69)

$$\begin{aligned}\langle \mathcal{Z}_V^n \rangle = \int \mathcal{D}[\phi] \exp\Bigg[-\frac{1}{2}\int \mathrm{d}^d x \ \sum_{j=1}^{n} \phi_j(\mathbf{x}) \left(\mathcal{F}^{-1}\left\{\mathcal{E}(\mathbf{k})\hat{\phi}(\mathbf{k})\right\}(\mathbf{x}) - E\phi_j(\mathbf{x})\right) \\ + \frac{w^2}{8}\int \mathrm{d}^d x \mathrm{d}^d y \ \phi^2(\mathbf{x}) C(\mathbf{x}-\mathbf{y}) \phi^2(\mathbf{y})\Bigg],\end{aligned} \tag{2.104}$$

where $\phi^2(\mathbf{x}) \equiv \sum_{j=1}^n \phi_j^2(\mathbf{x})$.

When rescaling the variables to make the equation unitless however the length by which I want to rescale the position will depend on the exact shape of $\mathcal{E}(\mathbf{k})$. The reason for rescaling in the first place is to make the instanton equation analytically simple. In particular for the parabolic case I rescaled the length to give the same coefficient for both terms quadratic in ϕ in Eq. 2.104, and I want to do a similar procedure for a general dispersion relation.

Note that when rescaling the position $\mathbf{x}$ by a factor l I also have to rescale the wave vector $\mathbf{k}$ by a factor of l^{-1} to keep $\mathbf{k}\cdot\mathbf{x}$ invariant in the Fourier transform. Rescaling $\mathbf{x} \mapsto l\mathbf{x}$ thus means rescaling the dispersion relation $\mathcal{E}(\mathbf{k}) \mapsto \mathcal{E}(\mathbf{k}/l)$. Defining a unitless dispersion relation $\tilde{\mathcal{E}}$ through

$$|E|\tilde{\mathcal{E}}(\mathbf{k}) = \mathcal{E}(\mathbf{k}/l) \implies \tilde{\mathcal{E}}(\mathbf{k}) = \mathcal{E}(\mathbf{k}/l)/|E|, \tag{2.105}$$

rescaling gives the general equivalent to Eq. 2.70

$$\begin{aligned}&\sum_{j=1}^n \phi_j(\mathbf{x}) \left(\mathcal{F}^{-1}\left\{\mathcal{E}(\mathbf{k})\hat{\phi}(\mathbf{k})\right\}(\mathbf{x}) - E\phi_j(\mathbf{x})\right)\\ &\mapsto \sum_{j=1}^n \phi_j(\mathbf{x}) \left(|E|\mathcal{F}^{-1}\left\{\tilde{\mathcal{E}}(\mathbf{k})\hat{\phi}(\mathbf{k})\right\}(\mathbf{x}) + |E|\phi_j(\mathbf{x})\right).\end{aligned} \tag{2.106}$$

Clearly exactly which factor l that is useful will depend on the dispersion relation, so I will go into more detail about this choice when I have actually chosen specific dispersion relations to work with.

Calculating the instanton equation is done in the same way as in subsection 2.5.2, although I now have to prove that (compare with Eq. 2.87)

$$\frac{\delta}{\delta\phi_k(\mathbf{x})}\left(\int \mathrm{d}^d y \ \sum_{j=1}^n \phi_j(\mathbf{y})\frac{1}{2}\mathcal{F}^{-1}\left\{\tilde{\mathcal{E}}(\mathbf{k})\hat{\phi}_j(\mathbf{k})\right\}(\mathbf{y})\right) = \mathcal{F}^{-1}\left\{\tilde{\mathcal{E}}(\mathbf{k})\hat{\phi}_j(\mathbf{k})\right\}(\mathbf{x}). \tag{2.107}$$

First note that

$$\frac{\delta}{\delta\phi_k(\mathbf{x})}\hat{\phi}_j(\mathbf{k}) = \frac{\delta}{\delta\phi_k(\mathbf{x})}\int \mathrm{d}^d y \ \phi_j(\mathbf{y})e^{-i\mathbf{k}\cdot\mathbf{y}} = \delta_{kj}e^{-i\mathbf{k}\cdot\mathbf{x}}. \tag{2.108}$$

Thus

$$\begin{aligned}&\frac{\delta}{\delta\phi_k(\mathbf{x})}\mathcal{F}^{-1}\left\{\tilde{\mathcal{E}}(\mathbf{k})\hat{\phi}_j(\mathbf{k})\right\}(\mathbf{y}) = \frac{\delta}{\delta\phi_k(\mathbf{x})}\frac{1}{2\pi}\int \mathrm{d}^d k \ \tilde{\mathcal{E}}(\mathbf{k})\hat{\phi}_j(\mathbf{k})e^{i\mathbf{k}\cdot\mathbf{y}} =\\ &= \delta_{kj}\frac{1}{2\pi}\int \mathrm{d}^d k \ \tilde{\mathcal{E}}(\mathbf{k})e^{-i\mathbf{k}\cdot\mathbf{x}}e^{i\mathbf{k}\cdot\mathbf{y}} = \delta_{kj}\frac{1}{2\pi}\int \mathrm{d}^d k \ \tilde{\mathcal{E}}(\mathbf{k})e^{i\mathbf{k}\cdot(\mathbf{y}-\mathbf{x})} =\\ &= \delta_{kj}\frac{1}{2\pi}\int \mathrm{d}^d k \ \tilde{\mathcal{E}}(\mathbf{k})e^{i\mathbf{k}\cdot(\mathbf{x}-\mathbf{y})},\end{aligned} \tag{2.109}$$

where I used $\tilde{\mathcal{E}}(\mathbf{k}) = \tilde{\mathcal{E}}(-\mathbf{k})$. It then follows that

$$\begin{aligned}&\int \mathrm{d}^d y \ \sum_{j=1}^n \phi_j(\mathbf{y})\left(\frac{\delta}{\delta\phi_k(\mathbf{x})}\mathcal{F}^{-1}\left\{\tilde{\mathcal{E}}(\mathbf{k})\hat{\phi}_j(\mathbf{k})\right\}(\mathbf{y})\right)\\ &= \frac{1}{2\pi}\int \mathrm{d}^d y\mathrm{d}^d k \ \phi_k(\mathbf{y})\tilde{\mathcal{E}}(\mathbf{k})e^{i\mathbf{k}\cdot(\mathbf{x}-\mathbf{y})} = \frac{1}{2\pi}\int \mathrm{d}^d k \ \hat{\phi}_k(\mathbf{k})\tilde{\mathcal{E}}(\mathbf{k})e^{i\mathbf{k}\cdot\mathbf{x}}\\ &= \mathcal{F}^{-1}\left\{\tilde{\mathcal{E}}(\mathbf{k})\hat{\phi}_k(\mathbf{k})\right\}(\mathbf{x})\end{aligned} \tag{2.110}$$

Using this gives

$$\begin{aligned}
&\frac{\delta}{\delta\phi_k(\mathbf{x})}\left(\int \mathrm{d}^d y \ \sum_{j=1}^{n}\phi_j(\mathbf{y})\frac{1}{2}\mathcal{F}^{-1}\left\{\tilde{\mathcal{E}}(\mathbf{k})\hat{\phi}_j(\mathbf{k})\right\}(\mathbf{y})\right)\\
&=\frac{1}{2}\int \mathrm{d}^d y \ \sum_{j=1}^{n}\left(\frac{\delta}{\delta\phi_k(\mathbf{x})}\phi_j(\mathbf{y})\right)\mathcal{F}^{-1}\left\{\tilde{\mathcal{E}}(\mathbf{k})\hat{\phi}_j(\mathbf{k})\right\}(\mathbf{y})\\
&\qquad+\frac{1}{2}\int \mathrm{d}^d y \ \sum_{j=1}^{n}\phi_j(\mathbf{y})\left(\frac{\delta}{\delta\phi_k(\mathbf{x})}\mathcal{F}^{-1}\left\{\tilde{\mathcal{E}}(\mathbf{k})\hat{\phi}_j(\mathbf{k})\right\}(\mathbf{y})\right)=\\
&=\frac{1}{2}\mathcal{F}^{-1}\left\{\tilde{\mathcal{E}}(\mathbf{k})\hat{\phi}_k(\mathbf{k})\right\}(\mathbf{x})+\frac{1}{2}\mathcal{F}^{-1}\left\{\tilde{\mathcal{E}}(\mathbf{k})\hat{\phi}_k(\mathbf{k})\right\}(\mathbf{x})\\
&=\mathcal{F}^{-1}\left\{\tilde{\mathcal{E}}(\mathbf{k})\hat{\phi}_k(\mathbf{k})\right\}(\mathbf{x})
\end{aligned}\tag{2.111}$$

Proceeding as in section 2.5.2, I arrive at the instanton solution $\vec{\phi}(\mathbf{x})=\hat{n}f(\mathbf{x})$, where $f(\mathbf{x})$ satisfies the instanton equation

$$\mathcal{F}^{-1}\left\{\tilde{\mathcal{E}}(\mathbf{k})\hat{f}^{\star}(\mathbf{k})\right\}(\mathbf{x})+f^{\star}(\mathbf{x})=f^{\star}(\mathbf{x})\int \mathrm{d}^d y \ (f^{\star})^2(\mathbf{y})C_{\lambda}(\mathbf{x}-\mathbf{y}),\tag{2.112}$$

l with the action of the instanton solution still given by 2.95.

3

Numerical Solution of the Instanton Equation

In this chapter I discuss the numerical method used to solve the instanton equation Eq. 2.112. Solving this is not straightforward. The instanton equation defines a local relation at every spatial point, but the equation itself depends on the whole function $f(\mathbf{x})$, and furthermore the only boundary for the equation are that it goes to 0 at infinity. Solvers based on initial values are therefore ill-fitted for the problem.

The method I have used that can handle these problems is a slightly modified version of the spectral renormalization method described by Ablowitz and Musslimani [12]. Using this method one can create an iterative scheme that finds the Fourier transform of the solution. To start, consider the Fourier transform of the instanton equation Eq. 2.112

$$\tilde{\mathcal{E}}(\mathbf{k})\hat{f}(\mathbf{k}) + \hat{f}(\mathbf{k}) = \mathcal{F}\left\{f(\mathbf{x})\int \mathrm{d}^d y \;\; f^2(\mathbf{y})C_\lambda(\mathbf{x}-\mathbf{y})\right\}(\mathbf{k}), \tag{3.1}$$

where the Fourier transform $\mathcal{F}$ is given by Eq. 2.98 and the unitless dispersion $\mathcal{E}$ by Eq. 2.105. Dividing both sides of the equation by $\tilde{\mathcal{E}}(\mathbf{k}) + 1$, gives the relation

$$\hat{f}(\mathbf{k}) = \frac{1}{\tilde{\mathcal{E}}(\mathbf{k}) + 1}\mathcal{F}\left\{f(\mathbf{x})\int \mathrm{d}^d y \;\; f^2(\mathbf{y})C(\mathbf{x}-\mathbf{y})\right\}(\mathbf{k}). \tag{3.2}$$

Note that the left-hand side of the equation is linear in f, while the right-hand side is cubic in f. Writing $f(\mathbf{x}) = \mu g(\mathbf{x})$, where μ is a real number thus gives

$$\hat{g}(\mathbf{k}) = \frac{\mu^2}{\tilde{\mathcal{E}}(\mathbf{k}) + 1}\mathcal{F}\left\{g(\mathbf{x})\int \mathrm{d}^d y \;\; g^2(\mathbf{y})C(\mathbf{x}-\mathbf{y})\right\}(\mathbf{k}). \tag{3.3}$$

Now, if one can find a function g and a constant μ that satisfies equation 3.3 then extracting f is trivial. So far this has just been a trivial rescaling of the function but as it turns out it is possible to construct an iterative scheme for approximating g and μ. The idea behind this is the following: Eq. 3.3 gives a local relation between $\hat{g}(\mathbf{k})$ and μ at each point in $\mathbf{k}$-space. Furthermore integrating both sides of Eq. 3.3

gives

$$\int \mathrm{d}^d k\ \hat{g}(\mathbf{k})\hat{g}^*(\mathbf{k}) = \int \mathrm{d}^d k\ \frac{\mu^2}{\tilde{\mathcal{E}}(\mathbf{k})+1}\mathcal{F}\left\{g(\mathbf{x})\int \mathrm{d}^d y\ g^2(\mathbf{y})C(\mathbf{x}-\mathbf{y})\right\}(\mathbf{k})\hat{g}^*(\mathbf{k}) \implies \tag{3.4}$$

$$\implies \mu^2 = \left(\int \mathrm{d}^d k\ \hat{g}(\mathbf{k})\hat{g}^*(\mathbf{k})\right) \Big/ \left(\int \mathrm{d}^d k\ \frac{1}{\tilde{\mathcal{E}}(\mathbf{k})+1}\mathcal{F}\left\{g(\mathbf{x})\int \mathrm{d}^d y\ g^2(\mathbf{y})C(\mathbf{x}-\mathbf{y})\right\}(\mathbf{k})\hat{g}^*(\mathbf{k})\right) \tag{3.5}$$

This allows the use of an iterative scheme through

$$\mu_n = \sqrt{\left(\int \mathrm{d}^d k\ \hat{g}_n(\mathbf{k})\hat{g}_n^*(\mathbf{k})\right) \Big/ \left(\int \mathrm{d}^d k\ \frac{1}{\tilde{\mathcal{E}}(\mathbf{k})+1}\mathcal{F}\left\{g_n(\mathbf{x})\int \mathrm{d}^d y\ g_n^2(\mathbf{y})C(\mathbf{x}-\mathbf{y})\right\}(\mathbf{k})\hat{g}_n^*(\mathbf{k})\right)} \tag{3.6}$$

$$\hat{g}_{n+1} = \frac{\mu_n^2}{\tilde{\mathcal{E}}(\mathbf{k})+1}\mathcal{F}\left\{g_n(\mathbf{x})\int \mathrm{d}^d y\ g_n^2(\mathbf{y})C(\mathbf{x}-\mathbf{y})\right\}(\mathbf{k}), \tag{3.7}$$

starting from some initial guess g_0. Note however that if there are values $\mathbf{k}$ for which $\tilde{\mathcal{E}}(\mathbf{k})+1 = 0$, then one cannot simply divide by $\tilde{\mathcal{E}}(\mathbf{k})+1$. This can be resolved by adding an extra term in the equation. As I have previously discussed however $\tilde{\mathcal{E}}(\mathbf{k})$ must possess some minimum, which I will call $\tilde{\mathcal{E}}_0$. Let r be a constant with $r > |\tilde{\mathcal{E}}_0| \implies r+\tilde{\mathcal{E}}_0 > 0$. Adding this to both sides of Eq. 3.1 gives

$$\tilde{\mathcal{E}}(\mathbf{k})\hat{f}(\mathbf{k}) + \hat{f}(\mathbf{k}) + r\hat{f}(\mathbf{k}) = \mathcal{F}\left\{f(\mathbf{x})\int \mathrm{d}^d y\ f^2(\mathbf{y})C_\lambda(\mathbf{x}-\mathbf{y})\right\}(\mathbf{k}) + r\hat{f}(\mathbf{k}), \tag{3.8}$$

which implies

$$\hat{f}(\mathbf{k}) = \frac{1}{\tilde{\mathcal{E}}(\mathbf{k})+r+1}\left(\mathcal{F}\left\{f(\mathbf{x})\int \mathrm{d}^d y\ f^2(\mathbf{y})C(\mathbf{x}-\mathbf{y})\right\}(\mathbf{k}) + r\hat{f}(\mathbf{k})\right). \tag{3.9}$$

Constructing an iterative scheme as before by splitting $f(\mathbf{x}) = \mu g(\mathbf{x})$ from this equation instead gives

$$\mu_n = \sqrt{\frac{\int \mathrm{d}^d k\ \hat{g}_n(\mathbf{k})\hat{g}_n^*(\mathbf{k})\dfrac{\tilde{\mathcal{E}}(\mathbf{k})+1}{\tilde{\mathcal{E}}(\mathbf{k})+r+1}}{\int \mathrm{d}^d k\ \dfrac{1}{\tilde{\mathcal{E}}(\mathbf{k})+r+1}\mathcal{F}\left\{g_n(\mathbf{x})\int \mathrm{d}^d y\ g_n^2(\mathbf{y})C(\mathbf{x}-\mathbf{y})\right\}(\mathbf{k})\hat{g}_n^*(\mathbf{k})}} \tag{3.10}$$

$$\hat{g}_{n+1} = \frac{1}{\tilde{\mathcal{E}}(\mathbf{k})+r+1}\left(\mu_n^2\mathcal{F}\left\{g_n(\mathbf{x})\int \mathrm{d}^d y\ g_n^2(\mathbf{y})C(\mathbf{x}-\mathbf{y})\right\}(\mathbf{k}) + r\hat{g})(\mathbf{k})\right), \tag{3.11}$$

which avoids dividing by zero and reduces to the previous scheme when $r = 0$.

4

Solutions to the Instanton Equation

In this chapter I will discuss the solutions to the instanton equation for different band structures. First I will discuss the results for parabolic dispersions, which have been investigated historically, and show how one can solve it analytically for energies deep in the tail. I will then move on and present the generalization to monomial dispersion relations $\mathcal{E}(\mathbf{k}) \propto |\mathbf{k}|^q$, where q is a positive integer.

4.1 Instanton solution for parabolic dispersions

Although the instanton equation is quite complicated, in a few cases it is actually analytically solvable. One such case is parabolic dispersions with $\lambda \gg 1$. Since the parameter $\lambda \propto \sqrt{|E|}$, this implies that the energy $|E|$ is deep in the tail. The results in this section were derived by me, afterwards I discovered that the same result had already been found [13].

Starting from the instanton equation for a parabolic dispersion 2.94 one can use the ansatz $f(\mathbf{x}) = ae^{-|\mathbf{x}|^2/2l^2}$. Now, for the k:th spatial dimension the second derivative in that direction is given by

$$\partial_k^2 f(\mathbf{x}) = \left(\frac{x_k^2}{l^4} - \frac{1}{l^2}\right) f(\mathbf{x}), \tag{4.1}$$

where x_k is the k:th component of $\mathbf{x}$. Summing over all components gives

$$\nabla^2 f(\mathbf{x}) = \left(\frac{|\mathbf{x}|^2}{l^4} - \frac{d}{l^2}\right) f(\mathbf{x}). \tag{4.2}$$

Furthermore

$$\begin{aligned}\int \mathrm{d}^d y f^2(\mathbf{y}) C(\mathbf{x}-\mathbf{y}) &= a^2(\pi\lambda^2)^{-d/2} \int \mathrm{d}^d y \exp\left[-\frac{|\mathbf{y}|^2}{l^2} - \frac{|\mathbf{x}-\mathbf{y}|^2}{\lambda^2}\right] \\ &= a^2(\pi\lambda^2)^{-d/2} \int \mathrm{d}^d y \exp\left[\sum_{k=1}^{d}\left(-\frac{y_k^2}{l^2} - \frac{(x_k-y_k)^2}{\lambda^2}\right)\right].\end{aligned} \tag{4.3}$$

The integrals in each spatial dimension can then be performed separately. Using the one dimensional integral

$$\int_{-\infty}^{\infty} \mathrm{d}y \exp\left[-\frac{y^2}{l^2} - \frac{(x-y)^2}{\lambda^2}\right] = \sqrt{\frac{\pi l^2 \lambda^2}{l^2+\lambda^2}} \exp\left[-\frac{x^2}{l^2+\lambda^2}\right], \tag{4.4}$$

the integral thus becomes

$$\begin{aligned}\int \mathrm{d}^d y f^2(\mathbf{y}) C(\mathbf{x}-\mathbf{y}) &= a^2(\pi\lambda^2)^{-d/2}\left(\frac{\pi l^2\lambda^2}{l^2+\lambda^2}\right)^{d/2} \exp\left[-\frac{|\mathbf{x}|^2}{l^2+\lambda^2}\right] \\ &= a^2\left(\frac{l^2}{l^2+\lambda^2}\right)^{d/2} \exp\left[-\frac{|\mathbf{x}|^2}{l^2+\lambda^2}\right].\end{aligned} \tag{4.5}$$

Now, assuming that $l \ll \lambda$, then over the majority of the volume of $f(\mathbf{x})$ one can approximate $\exp\left[-\frac{|\mathbf{x}|^2}{l^2+\lambda^2}\right] \approx 1 - \frac{|\mathbf{x}|^2}{l^2+\lambda^2}$. Then the differential equation reads

$$\left(\frac{|\mathbf{x}|^2}{l^4} - \frac{d}{l^2}\right) f(\mathbf{x}) = f(\mathbf{x}) - f(\mathbf{x}) a^2 \left(\frac{l^2}{l^2+\lambda^2}\right)^{d/2} \left(1 - \frac{|\mathbf{x}|^2}{l^2+\lambda^2}\right). \tag{4.6}$$

Dividing by $f(\mathbf{x})$ and equating the two sides gives the conditions

$$-\frac{d}{l^2} = 1 - a^2\left(\frac{l^2}{l^2+\lambda^2}\right)^{d/2} \implies a^2\left(\frac{l^2}{l^2+\lambda^2}\right)^{d/2} = 1 + \frac{d}{l^2}, \tag{4.7}$$

and

$$\begin{aligned}\frac{|\mathbf{x}|^2}{l^4} = a^2\left(\frac{l^2}{l^2+\lambda^2}\right)^{d/2} \frac{|\mathbf{x}|^2}{l^2+\lambda^2} &= \left(1 + \frac{d}{l^2}\right)\frac{|\mathbf{x}|^2}{l^2+\lambda^2} \\ \implies l^2 + \lambda^2 &= l^4 + d \cdot l^2 \\ \implies l &= \sqrt{\sqrt{\lambda^2 + \left(\frac{d-1}{2}\right)^2} - \frac{d-1}{2}},\end{aligned} \tag{4.8}$$

which is the only real positive root of the equation. For large values of λ, $l \approx \sqrt{\lambda}$. The correlation moment then becomes

$$\begin{aligned}S[f^\star] &= \int \mathrm{d}^d x \mathrm{d}^x y f^2(\mathbf{y}) C(\mathbf{x}-\mathbf{y}) f^2(\mathbf{x}) = \int \mathrm{d}^d x f^2(\mathbf{x}) \left(\int \mathrm{d}^d y f^2(\mathbf{y}) C(\mathbf{x}-\mathbf{y})\right) \\ &= \int \mathrm{d}^d x a^2 \exp\left[-\frac{|\mathbf{x}|^2}{l^2}\right] a^2 \left(\frac{l^2}{l^2+\lambda^2}\right)^{d/2} \exp\left[-\frac{|\mathbf{x}|^2}{l^2+\lambda^2}\right] \\ &= a^4\left(\frac{l^2}{l^2+\lambda^2}\right)^{d/2} \cdot \left(\pi l^2 \frac{l^2+\lambda^2}{2l^2+\lambda^2}\right)^{d/2} \\ &= a^4\left(\pi \frac{l^4}{2l^2+\lambda^2}\right)^{d/2}\end{aligned} \tag{4.9}$$

Since $a \approx \lambda^{d/4}$ and $l \approx \lambda^{1/2}$ for large λ, we see that for $\lambda >> 1$ the action $S[f^\star] \approx \pi^{d/2}\lambda^d$.

In Figure 4.1 I compare the theoretical instanton action with simulations, and one can see that it agrees for large correlation lengths for d = 1. These were calculated using the numerical algorithm described in Chapter 3.

Here there are two limits of the instanton action. For $\lambda \ll 1$ the correlation function behaves approximately as a delta function, and varies very slowly with energy. As λ grows however, it enters into a regime where the instanton solution can be approximated as a Gaussian, and thus the instanton action grows as $\pi^{d/2}\lambda^d$. All in all, for large values of $|E|$ density of states will approximately be

$$\exp\Big[-gS[\phi^\star]\Big] \approx \exp\left[-\frac{2|E|^2}{w^2}\left(\frac{\hbar^2}{2m|E|}\right)^{3/2}\left(\pi\lambda^2\right)^{d/2}\right] = \exp\left[-\frac{2|E|^2}{w^2}\left(\pi\lambda_0^2\right)^{d/2}\right]. \tag{4.10}$$

Physically, these limits can be understood in the following way: States probe lengths related to their de Broglie wavelength, which is inversely proportional to the magnitude of their energy. States with very small energies thus probe very large distances. As long as this distance is very large compared to the physical correlation length of the disorder potential $V(\mathbf{x})$, these states experience the disorder potential as being rapidly fluctuating and essentially acting as a uncorrelated random potential. This enters in the calculations through the effective correlation length $\lambda \propto \sqrt{|E|}$, where small $|E|$ imply small λ and thus the effective correlation $C_\lambda(\mathbf{x}) \approx C_0(\mathbf{x}) = \delta(\mathbf{x})$. For these energies the bound states in different valleys of the disorder potential interfere heavily with each other.

For states deeper in the tail, with larger negative energies, the distance probed becomes shorter. When this distance becomes much shorter than the physical correlation length of the disorder potential, the states will experience it as being heavily correlated. For these energies the bound states in different valleys have a very small effect on each other, and thus the probabilty of finding a bound state at a certain energy will be proportional to the probability of such a peak existing in the first place, and thus the density of states will be proportional to $\exp\left[-\frac{2|E|^2}{w^2}\left(\pi\lambda_0^2\right)^{d/2}\right]$.

For solids with parabolic dispersions in three dimensions then the density of states for very small negative energies varies as $\log\rho(E) \propto -|E|^{2-3/2} = -|E|^{1/2}$, and for very large negative energies as $\log\rho(E) \propto -|E|^2$. Note however that the band tails measured in real materials usually take the form of purely exponential decays $\log\rho(E) \propto -|E|$ [1], and thus it seems that most of the observed band tails fall in the intermediate energy regions that interpolate between very small and very large negative energies.

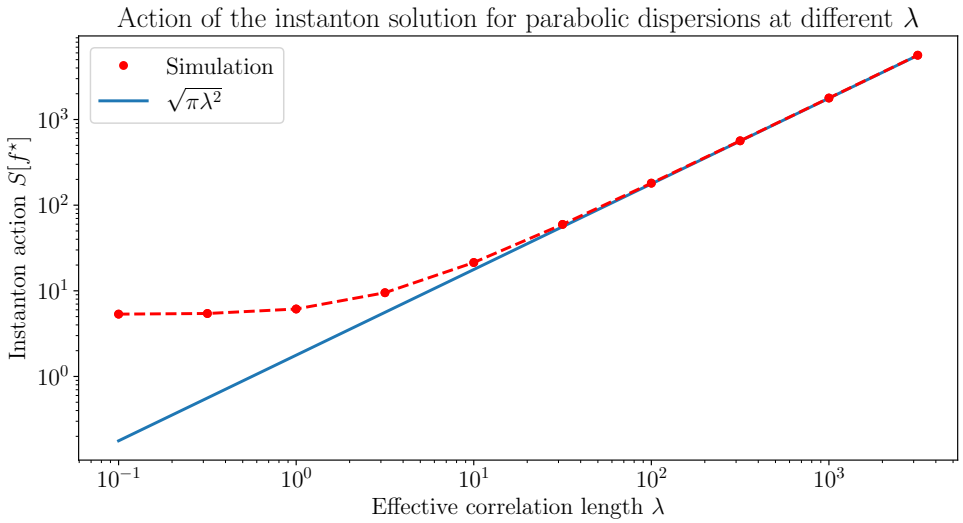

Figure 4.1: Action of the instanton solution for a parabolic dispersion as a function of the effective correlation length.

4.2 Correlated noise for higher-order dispersion relations

As I have shown it is possible to find analytic solutions to the instanton equation if the dispersion relation is parabolic. This is not always the case. In multilayer graphene for example, the low-energy band structure has a dispersion relation of the form $\mathcal{E}(\mathbf{k}) = \alpha|\mathbf{k}|^q$. In this section I analyze these types of band structures.

To start, one needs to look at what length-scale to pick to make the instanton equation unitless. For these simple monomial dispersion relations it is convient to rescale the length as $\mathbf{x} \mapsto (\alpha/|E|)^{1/q}\mathbf{x}$. The unitless dispersion relation will then be given by Eq. 2.105

$$\tilde{\mathcal{E}}(\mathbf{k}) = \mathcal{E}(\mathbf{k}/l)/|E| = \frac{\alpha}{|E|}\left(\frac{|E|^{1/q}}{\alpha^{1/q}}\mathbf{k}\right)^q = |\mathbf{k}|^q. \tag{4.11}$$

The instanton equation will thus be

$$\mathcal{F}^{-1}\left\{|\mathbf{k}|^q\hat{f}(\mathbf{k})\right\}(\mathbf{x}) + f(\mathbf{x}) = f(\mathbf{x})\int \mathrm{d}^d y\ f^2(\mathbf{y})C_\lambda(\mathbf{x}-\mathbf{y}). \tag{4.12}$$

For even q one can use the identity $\mathcal{F}^{-1}\left\{|\mathbf{k}|^q\hat{f}(\mathbf{k})\right\} = (-1)^{q/2}\nabla^q f(\mathbf{x})$ to write the instanton equation without any Fourier transform as

$$\pm\nabla^q f(\mathbf{x}) = f(\mathbf{x}) - f(\mathbf{x})\int \mathrm{d}^d y\ f^2(\mathbf{y})\frac{e^{-\frac{(\mathbf{x}-\mathbf{y})^2}{\lambda^2}}}{(\pi\lambda^2)^{d/2}}, \tag{4.13}$$

Although finding analytical solutions to the instanton equation with generic order terms may not even be possible, it is still possible under some assumptions to calculate the instanton action. In this derivation I will assume that q is even to be

able to write the kinetic term as a pure derivative, however numerical simulations indicates that the results hold for odd q as well.

Note that in the derivation for the instanton solution for parabolic dispersions 4.1, a key point that made it possible to express it analytically was that the width l of the solution was much smaller than the correlation length λ. When this is the case, the correlation function $C_\lambda(\mathbf{x})$ over most of the support of the instanton solution is almost constant.

This can be generalized this in the following way. Suppose there exists a function $w(\lambda)$ which contains most of the volume of $\int \mathrm{d}^d x |f(\mathbf{x})|$. Since the contributions to the instanton action outside this region are vanishingly small, it can be approximated as coming only from the points inside it. Furthermore, if $w(\lambda)$ grows much slower than λ, then the instanton equation in this region can be approximated by considering only the terms of the lowest order of λ in $C_\lambda(\mathbf{x})$, which allows a simplification of the instanton equation.

Let me now be a little more precise. Suppose there exists a function $w(\lambda)$ such that

$$\lim_{\lambda\to\infty} \frac{w(\lambda)}{\lambda} = 0 \text{ and } \lim_{\lambda\to\infty} \frac{\int_{\mathcal{B}_w} \mathrm{d}^d x \ f^2(\mathbf{x})}{\int \mathrm{d}^d x \ f^2(\mathbf{x})} = 1, \tag{4.14}$$

where $\mathcal{B}_w$ denotes a d-ball with radius $w(\lambda)$. Here $w(\lambda)$ can be interpreted as the width of the instanton solution, that is to say the radius of a ball which contains most of the integral volume which I assume grows much slower than λ. Note now that for $\mathbf{x}, \mathbf{y} \in \mathcal{B}_w$ the distance between any two points $\mathbf{x}, \mathbf{y}$ in this ball satisfies $|\mathbf{x}-\mathbf{y}| \leq 2w$. Using this one gets

$$\begin{aligned}\int_{\mathcal{B}_w} \mathrm{d}^d x \mathrm{d}^d y \ f^2(\mathbf{x}) f^2(\mathbf{y}) e^{-\frac{4w^2}{\lambda^2}} &\leq \int_{\mathcal{B}_w} \mathrm{d}^d x \mathrm{d}^d y \ f^2(\mathbf{x}) f^2(\mathbf{y}) e^{-\frac{(\mathbf{x}-\mathbf{y})^2}{\lambda^2}} \\ &\leq \int \mathrm{d}^d x \mathrm{d}^d y \ f^2(\mathbf{x}) f^2(\mathbf{y}) e^{-\frac{(\mathbf{x}-\mathbf{y})^2}{\lambda^2}} \leq \int \mathrm{d}^d x \mathrm{d}^d y \ f^2(\mathbf{x}) f^2(\mathbf{y})\end{aligned} \tag{4.15}$$

Dividing by $\int \mathrm{d}^d x \mathrm{d}^d y \ f^2(\mathbf{x}) f^2(\mathbf{y})$ gives

$$\begin{aligned}&\lim_{\lambda\to\infty} \left(\int_{\mathcal{B}_w} \mathrm{d}^d x \mathrm{d}^d y \ f^2(\mathbf{x}) f^2(\mathbf{y}) e^{-\frac{4w^2}{\lambda^2}} \right) \Big/ \left(\int \mathrm{d}^d x \mathrm{d}^d y \ f^2(\mathbf{x}) f^2(\mathbf{y}) \right) \\ &= \lim_{\lambda\to\infty} \left(\int_{\mathcal{B}_w} \mathrm{d}^d x \mathrm{d}^d y \ f^2(\mathbf{x}) f^2(\mathbf{y}) e^{-0} \right) \Big/ \left(\int \mathrm{d}^d x \mathrm{d}^d y \ f^2(\mathbf{x}) f^2(\mathbf{y}) \right) \\ &= \lim_{\lambda\to\infty} \left(\int_{\mathcal{B}_w} \mathrm{d}^d x \ f^2(\mathbf{x}) \right)^2 \Big/ \left(\int \mathrm{d}^d x \ f^2(\mathbf{x}) \right)^2 = 1.\end{aligned} \tag{4.16}$$

and trivially

$$\lim_{\lambda\to\infty} \left(\int \mathrm{d}^d x \mathrm{d}^d y \ f^2(\mathbf{x}) f^2(\mathbf{y}) \right) \Big/ \left(\int \mathrm{d}^d x \mathrm{d}^d y \ f^2(\mathbf{x}) f^2(\mathbf{y}) \right) = 1. \tag{4.17}$$

By the squeeze theorem this thus implies that

$$\lim_{\lambda\to\infty}\left(\int \mathrm{d}^d x \mathrm{d}^d y\ f^2(\mathbf{x}) f^2(\mathbf{y}) e^{-\frac{(\mathbf{x}-\mathbf{y})^2}{\lambda^2}}\right) \Big/ \left(\int \mathrm{d}^d x \mathrm{d}^d y\ f^2(\mathbf{x}) f^2(\mathbf{y})\right) = 1. \tag{4.18}$$

For large λ the instanton action will thus grow approximately as

$$\frac{1}{(\pi\lambda^2)^{d/2}} \int \mathrm{d}^d x \mathrm{d}^d y\ f^2(\mathbf{x}) f^2(\mathbf{y}) e^{-\frac{(\mathbf{x}-\mathbf{y})^2}{\lambda^2}} \approx \frac{1}{(\pi\lambda^2)^{d/2}} \left(\int \mathrm{d}^d x\ f^2(\mathbf{x})\right)^2. \tag{4.19}$$

Here, one can use the instanton equation to determine $\int \mathrm{d}^d x\ f^2(\mathbf{x})$. Remember that Eq. 4.14 essentially means that in the limit $\lambda \to \infty$ the only points that will contribute to the integral are the points $|\mathbf{x}| \leq w(\lambda)$. Applying the squeeze theorem again for these points gives

$$\int \mathrm{d}^d y\ f^2(\mathbf{y}) e^{-\frac{(\mathbf{x}-\mathbf{y})^2}{\lambda^2}} \approx \int \mathrm{d}^d y\ f^2(\mathbf{y}), \tag{4.20}$$

for large λ. Thus, for large λ the instanton equation for these points becomes approximately

$$\pm\nabla^n f(\mathbf{x}) = f(\mathbf{x}) - f(\mathbf{x}) \int \mathrm{d}^d y\ f^2(\mathbf{y}) \frac{e^{-\frac{(\mathbf{x}-\mathbf{y})^2}{\lambda^2}}}{(\pi\lambda^2)^{d/2}} \approx f(\mathbf{x}) - f(\mathbf{x}) \frac{1}{(\pi\lambda^2)^{d/2}} \int \mathrm{d}^d y\ f^2(\mathbf{y}). \tag{4.21}$$

Now, let $c(\lambda) \equiv \frac{1}{(\pi\lambda^2)^{d/2}} \int \mathrm{d}^d y\ f^2(\mathbf{y})$. The instanton equation thus reduces to

$$\pm\frac{\nabla^q f(\mathbf{x})}{f(\mathbf{x})} = (1 - c(\lambda)). \tag{4.22}$$

Here there are two possibilities. First, if $c(\lambda) \neq 1$ then the solution will in general be a linear combination of states of the form $e^{\boldsymbol{\alpha}\cdot\mathbf{x}}$, where $|\alpha|^q = \mp(1 - c(\lambda))$. However, these solutions will either be purely oscillatory, or have exponential growth in some direction. This means that the integral $\int \mathrm{d}^d y\ f^2(\mathbf{y})$ diverges, so this cannot be a solution. The only other possibility is thus that $c(\lambda) \to 1$, which means that

$$\frac{\nabla^n f(\mathbf{x})}{f(\mathbf{x})} \to 0. \tag{4.23}$$

More importantly, $c(\lambda) \to 1$ means that

$$\lim_{\lambda\to\infty} \frac{1}{(\pi\lambda^2)^{d/2}} \int \mathrm{d}^d y\ f^2(\mathbf{y}) = 1. \tag{4.24}$$

Thus the instanton action grows approximately as

$$\frac{1}{(\pi\lambda^2)^{d/2}} \left(\int \mathrm{d}^d x\ f^2(\mathbf{x})\right)^2 \approx \frac{1}{(\pi\lambda^2)^{d/2}} (\pi\lambda^2)^d = (\pi\lambda^2)^{d/2}. \tag{4.25}$$

Note that this result is the same for all degrees of the derivative! This agrees with the analytical and simulation result for $n = 2$ and $d = 1$ presented in the previous section, and it also agrees with $n = 4$ and $d = 1$, see figure 4.2.

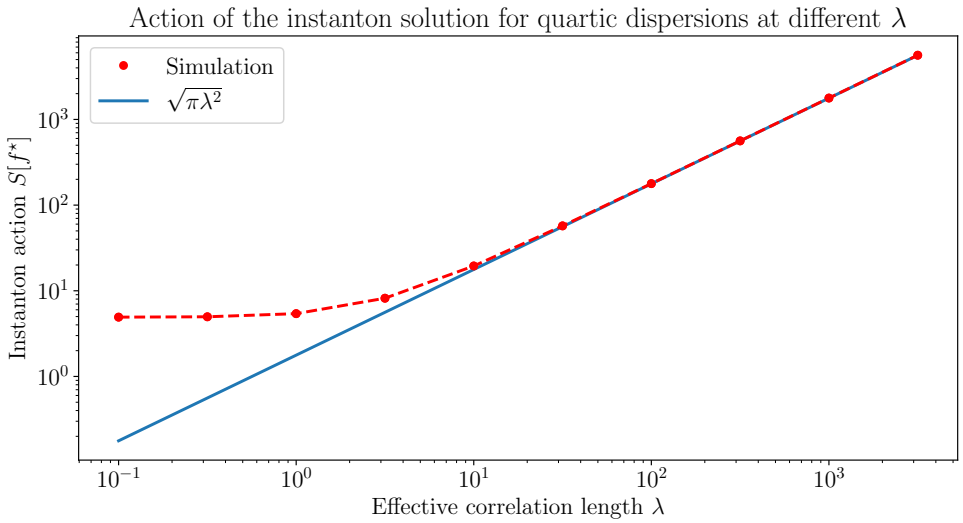

Figure 4.2: Instanton action for $n = 4$, $d = 1$ as a function of the correlation length λ.

In fact numerical simulations show that this relationship holds for both even and odd q up to 10 in $d = 1$.

Furthermore, combining this with the definition of g, for large energies the stationary point of the path integral will be

$$\exp\Big[-gS[\phi^\star]\Big] \approx \exp\left[-\frac{2|E|^2}{w^2}\left(\frac{\mu}{|E|}\right)^{d/q}\left(\pi\lambda^2\right)^{d/2}\right] = \exp\left[-\frac{2|E|^2}{w^2}\left(\pi\lambda_0^2\right)^{d/2}\right], \tag{4.26}$$

which is independent both of the order and of the "strength" of the kinetic term α, as long as the energy $|E|$ is large enough (i.e for energies deep in the tail). Just as for parabolic dispersions in this regime the electrons probe distances that are very short compared to the correlation length of the system, and the probability of finding a bound state at a certain energy will be proportional to the relative probability of such a bound state existing in the first place. Note however that this result does not include fluctuations, so the full disorder average presumably still depends on these quantities.

In three dimensions the density of states for monomial dispersion for very small energies is $\log\rho(E) \propto -|E|^{2-3/q}$, while for large energies it is $\log\rho(E) \propto -|E|^2$ just as for parabolic dispersions. This however presents an interesting point. Remember that most observed band tails are exponential $\log\rho(E) \propto -|E|$, which for parabolic dispersions $q = 2$ can be interpreted as the intermediate region which interpolates between $\log\rho(E) \propto -|E|^{1/2}$ and $\log\rho(E) \propto -|E|^2$. For $q > 2$ however, note that $p \equiv 2 - 3/q \geq 1$ for $q \geq 3$. Thus, band tails for monomial dispersions with powers $q \geq 3$ interpolate between the regions $\log\rho(E) \propto -|E|^p$, $p \geq 1$ and $\log\rho(E) \propto -|E|^2$. For these powers the purely exponential region seems to not exist at all!

Thus, this method predicts that band tails for monomial dispersions with a power

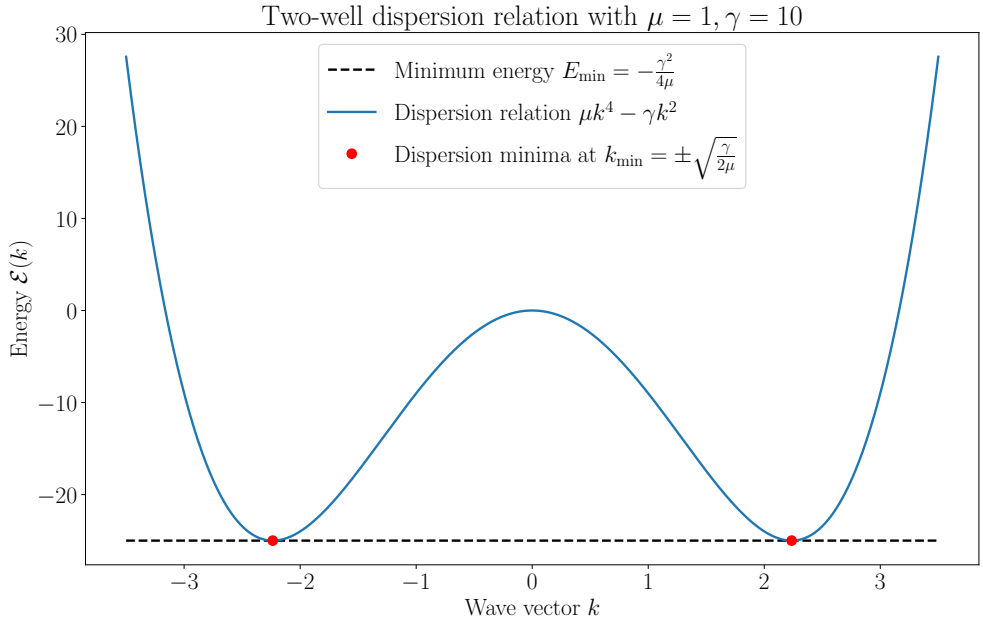

Figure 4.3: An example of a double-well dispersion and its minima.

$q > 2$ will not decay exponentially, but will decay with some larger factor. This suggests that a steeper dispersion may yield slightly smaller band tails.

4.3 Correlated terms for dispersions with multiple wells

Until now I have been looking at dispersion relations of the form $|\mathbf{k}|^q$, which have only a single zero at $\mathbf{k} = 0$. What happens for more complicated dispersions? To start, I will investigate the simplest one-dimensional case with two wells, with the kinetic term

$$H_0 = \mu\partial^4 + \gamma\partial^2, \tag{4.27}$$

corresponding to the dispersion relation

$$\mathcal{E}(k) = \mu k^4 - \gamma k^2. \tag{4.28}$$

Here I assume that $\mu, \gamma > 0$ giving a double-well band structure as can be seen in Figure 4.3. In this case since I have two terms in the dispersion relations I cannot normalize them both by rescaling the length, I can at most normalize one. In this case I choose to remove the fourth-order term by choosing $l = (|E|/\mu)^{1/4}$, giving the unitless dispersion relation

$$\tilde{\mathcal{E}}(k) = k^4 - \alpha k^2, \tag{4.29}$$

where $\alpha = \frac{\gamma}{\sqrt{\mu|E|}}$.

The instanton equation for Gaussian correlations is

$$\partial^4 f(x) + \alpha\partial^2 f(x) + f(x) = f(x)\int \mathrm{d}y\ f^2(y)\frac{e^{-\frac{(x-y)^2}{\lambda^2}}}{(\pi\lambda^2)^{1/2}}. \tag{4.30}$$

Thus, as the energy $|E|$ increases λ grows to infinity while α goes to zero. This means that the parabolic term in the dispersion becomes less and less important for energies deep in the tail. I will for the moment ignore this energy dependence and look at solutions to this equation as functions of α and λ. For $\alpha \geq 2$ numerical simulations only converge to the solution $f(\mathbf{x}) = 0$. The physical intuition for this is very simple. With the added term the lowest energy in the band will be $E_{\min} = -\frac{\gamma^2}{4\mu}$, which follows directly from minimizing $\mu|k|^4 - \gamma|k|^2$. Our definition of α implies that $\alpha \geq 2 \implies |E| \leq \frac{\gamma^2}{4\mu} = |E_{\min}|$. Thus, the instanton approximation breaks down for energies above the band, which is to be expected since these regions are dominated by the non-localized states.

For $0 < \alpha < 2$, the instanton solution will behave very differently from the case where $\alpha = 0$. To start, I will ignore the energy dependence of λ and α and instead vary them arbitrarily. For $\alpha = 0$ the instanton action grows approximately as $\sqrt{\pi\lambda^2}$, but for larger α it seems to grow instead as $(1 - \alpha^2/4)^2\sqrt{\pi\lambda^2}$, as can be seen in figure 4.4. Furthermore, the instanton solution for large λ seems to oscillate with the frequency $\sqrt{\alpha/2}$, which is precisely the minimum of the equation $k^4 - \alpha k^2$.

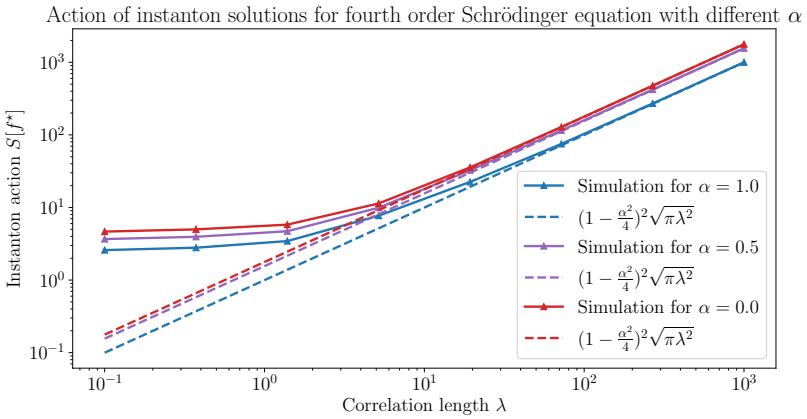

Figure 4.4: Instanton action for the dispersion relation $|k|^4 - \alpha|k|^2$.

It turns out that one can understand both of these phenomena analytically. Armed with the knowledge of the simulations, I use the ansatz that the instanton solution can be written as

$$f(x) = \cos(\omega x)g(x/l(\lambda)), \tag{4.31}$$

where ω is some angular frequency independent of λ, $g(x)$ is a profile that is also independent on λ and $l(\lambda)$ is a length scale that becomes larges as λ grows. For large values of λ then, higher order derivatives of $g(x/l(\lambda))$ will be suppressed compared to the derivatives of $\cos(\omega)$. Inserting this ansatz into the differential part of equation

4.30 gives

$$\begin{aligned}\partial^4 f(x) + \alpha\partial^2 f(x) = &\left(\omega^4 - \alpha\omega^2\right)\cos(\omega x)g(x/l) + \\ &+ \frac{1}{l}\left(4\omega^3 - 2\alpha\omega\right)\sin(\omega x)g'(x/l) + \\ &+ \frac{1}{l^2}\left(-6\omega^2 + \alpha\right)\cos(\omega x)g''(x/l) + \mathcal{O}(l^{-3}).\end{aligned} \tag{4.32}$$

Now, if $\omega = \sqrt{\alpha/2}$ as the simulations suggest then

$$\begin{aligned}\omega^4 - \alpha\omega^2 &= \frac{\alpha^2}{4} - \frac{\alpha^2}{2} = -\frac{\alpha^2}{2}, \\ 4\omega^3 - 2\alpha\omega &= 2\alpha\omega - 2\alpha\omega = 0, \\ -6\omega^2 + \alpha &= -\frac{6\alpha}{2} + \alpha = -\alpha.\end{aligned} \tag{4.33}$$

Thus

$$\partial^4 f(x) + \alpha\partial^2 f(x) = \left(-\frac{\alpha^2}{2}g(x/l) - \frac{1}{l^2}\alpha g''(x/l)\right)\cos(x\sqrt{\alpha/2}) + \mathcal{O}(l^{-3}). \tag{4.34}$$

Furthermore, assuming that $\cos(\omega x)$ varies much quicker than $g(x)$ then the following integral vanishes

$$\int \mathrm{d}y \;\; \cos(2\omega y)g^2(y) \approx 0, \tag{4.35}$$

since the oscillations cancel each other out. Since $\cos^2(x) = \frac{1}{2} + \frac{1}{2}\cos(2x)$ will thus have

$$\int \mathrm{d}y \;\; f^2(y)\frac{e^{-\frac{(x-y)^2}{\lambda^2}}}{(\pi\lambda^2)^{1/2}} \approx \frac{1}{2}\int \mathrm{d}y \;\; g^2(y/l)\frac{e^{-\frac{(x-y)^2}{\lambda^2}}}{(\pi\lambda^2)^{1/2}}. \tag{4.36}$$

All in all, inserting this ansatz into equation 4.30 gives approximately

$$\begin{aligned}&\left(-\frac{\alpha^2}{2}g(x/l) - \frac{1}{l^2}\alpha g''(x/l)\right)\cos(x\sqrt{\alpha/2}) + \cos(x\sqrt{\alpha/2})g(x/l) \\ &\approx \cos(x\sqrt{\alpha/2})g(x/l)\frac{1}{2}\int \mathrm{d}y \;\; g^2(y)\frac{e^{-\frac{(x-y)^2}{\lambda^2}}}{(\pi\lambda^2)^{1/2}}.\end{aligned} \tag{4.37}$$

Notice here that both sides are multiplied by a single factor of $\cos(x\sqrt{\alpha/2})$. Letting $g(x/l(\lambda)) \equiv h_\lambda(x)$, for all points where $\cos(x\sqrt{\alpha/2}) \neq 0$ thus gives the condition

$$\alpha\partial^2 h_\lambda(x) = \left(1 - \frac{\alpha^2}{2}\right)h_\lambda(x) - h_\lambda(x)\frac{1}{2}\int \mathrm{d}y \;\; h_\lambda^2(y)\frac{e^{-\frac{(x-y)^2}{\lambda^2}}}{(\pi\lambda^2)^{1/2}}. \tag{4.38}$$

But this is just a modified version of the Schrödinger instanton equation! By the same arguments as in section 4.2, we therefore expect the instanton action to ap-

proach

$$S[f^\star] = \int \mathrm{d}x\mathrm{d}y \;\; f_\lambda^2(x) \frac{e^{-\frac{(x-y)^2}{\lambda^2}}}{(\pi\lambda^2)^{1/2}} f_\lambda^2(y)$$

$$= \int \mathrm{d}x\mathrm{d}y \;\; \cos^2(x\sqrt{\alpha/2}) h_\lambda^2(x) \frac{e^{-\frac{(x-y)^2}{\lambda^2}}}{(\pi\lambda^2)^{1/2}} \cos^2(y\sqrt{\alpha/2}) h_\lambda^2(y) \approx \tag{4.39}$$

$$\approx \frac{1}{4} \frac{1}{(\pi\lambda^2)^{1/2}} \left(\int \mathrm{d}x \;\; h_\lambda^2(x) \right)^2 . \tag{4.40}$$

By the same arguments one can expect

$$\left(1 - \frac{\alpha^2}{2}\right) h_\lambda(x) - h_\lambda(x) \frac{1}{2} \int \mathrm{d}y \;\; h_\lambda^2(y) \frac{e^{-\frac{(x-y)^2}{\lambda^2}}}{(\pi\lambda^2)^{1/2}}$$

$$\approx \left(1 - \frac{\alpha^2}{2}\right) h_\lambda(x) - h_\lambda(x) \frac{1}{2} \int \mathrm{d}y \;\; h_\lambda^2(y) \frac{1}{(\pi\lambda^2)^{1/2}} \to 0$$

$$\implies \frac{1}{2} \int \mathrm{d}y \;\; h_\lambda^2(y) \to (\pi\lambda^2)^{1/2} \left(1 - \frac{\alpha^2}{2}\right) . \tag{4.41}$$

as λ grows, and thus one can expect

$$S[f^\star] \approx (\pi\lambda^2)^{1/2} \left(1 - \frac{\alpha^2}{2}\right)^2 , \tag{4.42}$$

for large values of λ, which is precisely the result of the numerical simulations, see figure 4.4.

4.3.1 Band tails for double-well dispersions

If one were to directly compare these results to the instanton action for monomial dispersions one might assume that the density of states for double-well dispersions are much larger than for monomial ones. However, there are a few details that must be taken into account when comparing these cases.

When looking at band tails the interesting energies are those below the minimum of the band, i.e in the gap. As I have previously mentioned though the minimum energy of the double-well dispersion is not zero but instead $E_{\min} = -\frac{\gamma^2}{4\mu}$. To meaningfully compare the tails for double-well dispersions with the tails for monomial dispersions, which have a minimum energy of zero, one needs to shift the energies of the double-well dispersion $E \mapsto E - E_{\min} = E + \frac{\gamma^2}{4\mu}$, so that the band minimum lies at $E = 0$ for both cases.

For large values of k the double-well dispersion will behave approximately as a simple fourth order dispersion $\mu k^4 - \gamma k^2 \approx \mu k^4$. Similarly, expanding the double-well dispersion around any of its two minima at $k_{\min} = \pm\sqrt{\frac{\gamma}{2\mu}}$ gives

$$\mu(k - k_{\min})^4 - \gamma(k - k_{\min})^2 = 2\gamma(k - k_{\min})^2 + \mathcal{O}((k - k_{\min})^3), \tag{4.43}$$

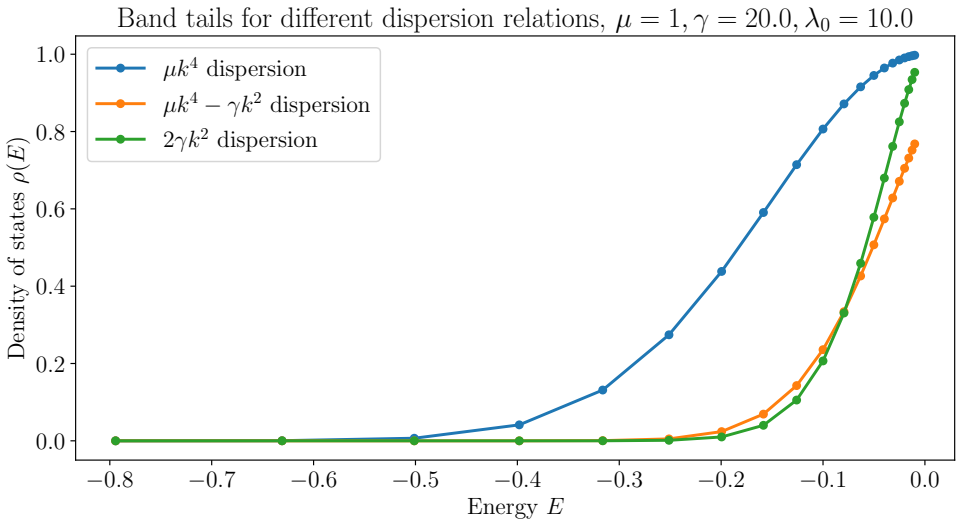

Figure 4.5: Band tails of the double-well dispersion $\mu k^4 - \gamma k^2$ as well as of the dispersions μk^4 and γk^2, with a relatively large value for γ.

so at the band minima the dispersion relation is approximately parabolic with a strength 2γ. A first guess as to the behaviour of the band tail is therefore that it behaves as the tail for a parabolic band for small $-E$ and transitions into the shape of a tail for a fourth-order dispersion as $E \to -\infty$.

Taking into account the shift in energies for the double-well dispersion, numerical simulations indicate that for certain parameter combinations the tail decays quicker than for the high-energy approximations. Comparing this to the low-energy approximations however suggests that double-well dispersions have larger widths than their low-energy approximations, as can be seen in Figures 4.6.

4.4 Summary and conclusion

To summarize, assuming a Gaussian correlated disorder potential, for monomial dispersions $\alpha|k|^q$ I have shown that the band tails exhibit two distinct regions depending on the effective correlation length $\lambda = \lambda_0/(\alpha/|E|)^{1/q}$. For $\lambda \ll 1$ the density of states is proportional to $\log \rho(E) \propto -|E|^{2-d/q}$, while for $\lambda \gg 1$ it is instead proportional to $\log \rho(E) \propto -|E|^2$. The purely exponential tails $\log \rho(E) \propto -|E|$ that have been observed in real solids seem to arise in the crossover region between these two limits.

Interestingly, this exponential crossover region cannot according to these calculation exist for monomial dispersions of power $q > 2$ in three dimensions, since the band tail for these dispersions will always decay quicker than a pure exponential decay. This suggests that materials with narrower minima may have shorter band tails. It also gives a way of validating the model I have used by measuring the band tails of more narrow dispersions.

For double-well dispersions in one dimension $\mu k^4 - \gamma k^2$ the dispersion for very small

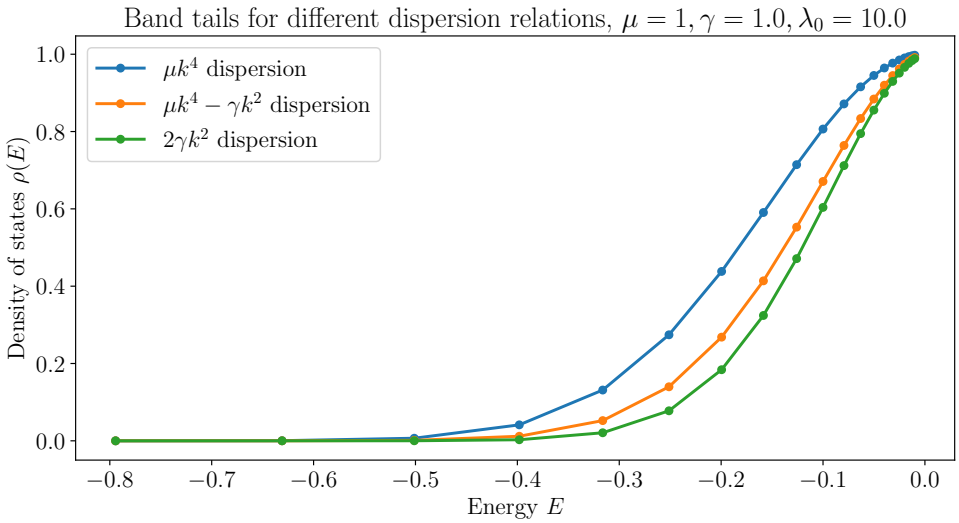

Figure 4.6: Band tails of the double-well dispersion $\mu k^4 - \gamma k^2$ as well as of the dispersions μk^4 and γk^2, with relatively equal values for μ and γ.

negative energies can be approximated by $2\gamma k^2$, while for large negative energies it can be approximated by μk^4. Numerical simulations seem to suggest that the band tails of double-well dispersions are narrower than their high-energy approximation but slighly wider than for the low-energy approximation. The double-well dispersion also qualitatively change how the band tails behave at the smaller energies by shifting all energy levels by a certain amount.

In conclusion I have shown that the shape of the band structure, i.e the dispersion relation can have a large effect on the shape of the band tails. Tentatively, my findings suggest that sharper minima seem to reduce the width of the band tails, while multiple peaks (at least in one dimension) seem to increase it.

Bibliography

[1] F. Urbach, "The long-wavelength edge of photographic sensitivity and of the electronic absorption of solids," *Phys. Rev.*, vol. 92, pp. 1324–1324, 5 Dec. 1953. DOI: 10.1103/PhysRev.92.1324. [Online]. Available: https://link.aps.org/doi/10.1103/PhysRev.92.1324.

[2] M. H. Cohen, M.-Y. Chou, E. N. Economou, S. John, and C. M. Soukoulis, "Band tails, path integrals, instantons, polarons, and all that," *IBM Journal of Research and Development*, vol. 32, no. 1, pp. 82–92, 1988. DOI: 10.1147/rd.321.0082.

[3] M. A. Khayer and R. K. Lake, "Effects of band-tails on the subthreshold characteristics of nanowire band-to-band tunneling transistors," *Journal of Applied Physics*, vol. 110, no. 7, Oct. 2011, 074508, ISSN: 0021-8979. DOI: 10.1063/1.3642954. [Online]. Available: https://doi.org/10.1063/1.3642954.

[4] J. Wong, S. T. Omelchenko, and H. A. Atwater, "Impact of semiconductor band tails and band filling on photovoltaic efficiency limits," *ACS Energy Letters*, vol. 6, no. 1, pp. 52–57, 2021. DOI: 10.1021/acsenergylett.0c02362.

[5] H. Min, "Electronic properties of multilayer graphene," in *Graphene Nanoelectronics: Metrology, Synthesis, Properties and Applications*, H. Raza, Ed. Berlin, Heidelberg: Springer Berlin Heidelberg, 2012, pp. 325–356, ISBN: 978-3-642-22984-8. DOI: 10.1007/978-3-642-22984-8_11. [Online]. Available: https://doi.org/10.1007/978-3-642-22984-8_11.

[6] S. John, M. Y. Chou, M. H. Cohen, and C. M. Soukoulis, "Density of states for an electron in a correlated gaussian random potential: Theory of the urbach tail," *Phys. Rev. B*, vol. 37, pp. 6963–6976, 12 Apr. 1988. DOI: 10.1103/PhysRevB.37.6963. [Online]. Available: https://link.aps.org/doi/10.1103/PhysRevB.37.6963.

[7] J. J. Sakurai and J. Napolitano, *Modern Quantum Mechanics*, 2nd ed. Cambridge University Press, 2017. DOI: 10.1017/9781108499996.

[8] P. Hofmann, *Solid State Physics: An Introduction*. Wiley, 2015, ISBN: 9783527682034. [Online]. Available: https://books.google.se/books?id=z6ycCQAAQBAJ.

[9] C. Nordling and J. Österman, *Physics Handbook for Science and Engineering*. Professional Publishing House, 2006, ISBN: 9789144044538. [Online]. Available: https://books.google.se/books?id=xBAWGQAACAAJ.

[10] T. Shinzato, *Validation of the replica trick for simple models*, 2016. arXiv: 1606.07277 [cond-mat.dis-nn].

[11] J. Zinn-Justin, *Quantum Field Theory and Critical Phenomena*. Oxford University Press, Jun. 2002, ISBN: 9780198509233. DOI: 10.1093/acprof:oso/

9780198509233.001.0001. [Online]. Available: https://doi.org/10.1093/acprof:oso/9780198509233.001.0001.

[12] M. J. Ablowitz and Z. H. Musslimani, "Spectral renormalization method for computing self-localized solutions to nonlinear systems," *Opt. Lett.*, vol. 30, no. 16, pp. 2140–2142, Aug. 2005. DOI: 10.1364/OL.30.002140. [Online]. Available: https://opg.optica.org/ol/abstract.cfm?URI=ol-30-16-2140.

[13] S. John and M. J. Stephen, "Electronic density of states in a long-range correlated potential," *Journal of Physics C: Solid State Physics*, vol. 17, no. 22, p. L559, Aug. 1984. DOI: 10.1088/0022-3719/17/22/004. [Online]. Available: https://dx.doi.org/10.1088/0022-3719/17/22/004.